

# Seasonally Optimized Calibrations Improve Low-cost Sensor Performance: Long-term Field Evaluation of PurpleAir Sensors in Urban and Rural India

Mark Joseph Campmier<sup>1</sup>, Jonathan Gingrich<sup>2</sup>, Saumya Singh<sup>1</sup>, Nisar Baig<sup>3</sup>, Shahzad Gani<sup>4, 5</sup>, Adithi Upadhyay<sup>6</sup>, Pratyush Agrawal<sup>7</sup>, Meenakshi Kushwaha<sup>6</sup>, Harsh Raj Mishra<sup>8</sup>, Ajay Pillarisetti<sup>9</sup>, Sreekanth Vakacherla<sup>7</sup>, Ravi Kant Pathak<sup>8,10</sup>, and Joshua S Apte<sup>1,9</sup>

<sup>1</sup>Department of Civil and Environmental Engineering, University of California, Berkeley, CA, 94720, USA

<sup>2</sup>Department of Engineering, Dordt University, Sioux Center, IA, 51250, USA

<sup>3</sup>Department of Civil Engineering, Indian Institute of Technology Delhi, New Delhi 110016, India

<sup>4</sup>Centre for Atmospheric Sciences, Indian Institute of Technology Delhi, New Delhi 110016, India

<sup>5</sup>Institute for Atmospheric and Earth System Research/Physics, University of Helsinki, Helsinki, 00100, Finland

<sup>6</sup>ILK Labs, Bengaluru, India

<sup>7</sup>Center for Study of Science, Technology and Policy, Bengaluru 560094, India

<sup>8</sup>Indo Gangetic Plains-Centre for Air Research and Education, Hamirpur 210301, India

<sup>9</sup>School of Public Health, University of California, Berkeley, CA 94720, USA

<sup>10</sup>Department of Chemistry and Molecular Biology, University of Gothenburg, Gothenburg, Sweden

**Correspondence:** Joshua S. Apte (apte@berkeley.edu)

**Abstract.** Lower-cost air pollution sensors can fill critical air quality data gaps in India, which experiences very high fine particulate matter (PM<sub>2.5</sub>) air pollution but has sparse regulatory air monitoring. Challenges for low-cost PM<sub>2.5</sub> sensors in India include high aerosol mass concentrations and pronounced regional and seasonal gradients in aerosol composition. Here, we report on a detailed long-time performance evaluation of a popular sensor, the Purple Air PA-II, at multiple sites in India.

5 We established 3 distinct sites in India across land-use categories and population density extremes (North India: Delhi [urban], Hamirpur [rural]; South India: Bangalore [urban]), where we collocated the PA-II with reference beta-attenuation monitors. We evaluated the performance of uncalibrated sensor data, and then developed, optimized, and evaluated calibration models using a comprehensive feature selection process with a view to reproducibility in the Indian context. We assessed the seasonal and spatial transferability of sensor calibration schemes, which is especially important in India because of the paucity of reference  
10 instrumentation. Without calibration, the PA-II was moderately correlated with the reference signal ( $R^2$ : 0.55 - 0.74) but was inaccurate ( $\text{NRMSE} \geq 40\%$ ). Relative to uncalibrated data, parsimonious annual calibration models improved PA performance at all sites (cross-validated  $\text{NRMSE}$  20-30%,  $R^2$ : 0.82-0.95), and greatly reduced seasonal and diurnal biases. Because aerosol properties and meteorology vary regionally, the form of these long-term models differed among our sites, suggesting that local calibrations are desirable when possible. Using a moving-window calibration, we found that using seasonally-specific  
15 information improves performance relative to a static annual calibration model, while a short-term calibration model generally does not transfer reliably to other seasons. Overall, we find that the PA-II can provide reliable PM<sub>2.5</sub> data with better than

±25% precision and accuracy when paired with a rigorous calibration scheme that accounts for seasonality and local aerosol composition.

## 1 Introduction

20 Exposure to fine particulate matter, or PM<sub>2.5</sub> (particles with aerodynamic diameter  $\leq 2.5 \mu\text{m}$ ), is a leading cause of adverse health outcomes, including premature death (Lepeule et al., 2012; Diseases and Collaborators, 2020). India experiences high mass concentrations in both its population-dense megacities and its rural areas, resulting in the largest number of deaths (about 0.98 million annual deaths, about 1.5 years reduction in life expectancy) attributable to ambient PM<sub>2.5</sub> worldwide (Apte et al., 2018; Collaborators, 2021). In particular New Delhi, the surrounding Delhi National Capital Region, and the broader Indo-  
25 Gangetic Plain of North India regularly experience hourly mass concentrations exceeding  $1000 \mu\text{g}/\text{m}^3$  (Gani et al., 2019) resulting in ill health effects even from short-term exposure (Gupta et al., 2021; Krishna et al., 2021). South India generally experiences lower PM<sub>2.5</sub> concentrations but still has population-weighted annual mass concentrations that exceed World Health Organization recommendations by a large margin (Apte and Pant, 2019). As relatively less polluted megacities in South India continue to rapidly grow, the challenge of ambient PM<sub>2.5</sub> will also increase (Guttikunda et al., 2019; Ramachandra et al., 2020).

30 Given the high exposure burden and complexity of PM<sub>2.5</sub> throughout India, there is a need to increase understanding of the spatial-temporal patterns of air pollution. Traditional regulatory monitors are expensive to install and maintain, requiring specialized teams and consistent power to maintain networks (Brauer et al., 2019). As a result, there is a dearth of monitors in India (Brauer et al., 2019; Martin et al., 2019). Although satellite remote sensing can fill in the spatial gap, it lacks high-quality temporal coverage and relies on ground-based monitoring for calibration algorithms (Hammer et al., 2020), which can, as is  
35 the case in India, result in biased estimates of surface PM<sub>2.5</sub> (Dey et al., 2020).

Starting in around 2010, advancements in miniaturized electronics and laser technology have resulted in the growth of low-cost (< 500 USD) PM<sub>2.5</sub> sensor technologies. These light-scattering monitors are popular within the research community and among citizen scientists. The company PurpleAir (PA) has been especially successful in developing (1) a 200-280 USD low-cost sensor that utilizes a commercially available, light-scattering sensor developed by Plantower (PMS5003) and (2) a  
40 platform for individuals and organizations to share data from indoor and outdoor PurpleAir low-cost sensor.

Light-scattering low-cost sensors require extensive data quality control and careful selection of calibration models to offer measurements comparable to reference quality instruments (Hagan and Kroll, 2020; Hagler et al., 2018). Optical sensors inaccurately estimate mass from aerosol scattering properties, since PM<sub>2.5</sub> is a mixture of particle sizes and chemical compositions thus resulting in spatial-temporal variability in optical properties (Hagan and Kroll, 2020; Levy Zamora et al., 2019; Zou et al.,  
45 2021). The roles of relative humidity, mass concentration range, sensor aging, and diverse source profiles have been extensively studied in laboratories and field conditions in the US, Australia, and Europe. Lab studies report the Plantower sensors do not adequately characterize fine particles above 0.8 microns (Kuula et al., 2020), deteriorate under extreme mass concentrations (Mehadi et al., 2020; Tryner et al., 2020), and are vulnerable to overestimation at RH greater than 60% (Jayaratne et al., 2018).

Field studies in low to moderate pollution environments show PA units can be calibrated to reference instruments using simple empirical regression techniques with environmental variables (Barkjohn et al., 2021; Malings et al., 2019; Zheng et al., 2018). Models are often specific to a season and location, however, Barkjohn et al. (2021) demonstrated that a continental US calibration equation could be effectively deployed for daily data.

Recently there is increased interest in understanding low-cost sensor performance in the Global South to fill major monitoring gaps (Bai et al., 2020; Jha et al., 2021; Malyan et al., 2023; McFarlane et al., 2021; Puttaswamy et al., 2022; Sreekanth et al., 2022; Zheng et al., 2018, 2019). In North India, Zheng et al. (2018) deployed Plantower models in Kanpur, Uttar Pradesh, for 90 days and found multilinear regression improved Plantower performance, albeit with significant error for hourly data. In South India, Puttaswamy et al. (2022) calibrated Plantower units for 68-days in Chennai and found a multilinear regression approach reduced uncertainty to within 15% and 18% for PM<sub>2.5</sub> and PM<sub>10</sub> respectively. Low-cost sensor studies in India report the importance of climate and emissions variability on aerosol characteristics and advise future deployments to test calibration algorithms across longer timelines (Malyan et al., 2023; Puttaswamy et al., 2022; Sreekanth et al., 2022; Zheng et al., 2018, 2019).

In this study, we deployed and evaluated PurpleAir PA-II sensors in Delhi, Hamirpur, and Bangalore by collocating with regulatory-grade instruments for 335, 154, and 312 days respectively. We built hourly local calibration models using multilinear regression. With proper data quality constraints, a relatively simple calibration model can produce high accuracy and low bias data. Despite this success, model performance degrades when attempting to transfer a model trained in each environment to data collected in a dissimilar environment. We found a more pronounced reduction in performance when attempting to transfer a model trained in one season to another season, as aerosol characteristics can shift rapidly even at the same site. Our work demonstrates low-cost sensors are a viable option for measuring spatial-temporal trends throughout India, but calibration models are vulnerable to the local and seasonal effects on aerosol properties.

## 2 Methods

### 2.1 Low-cost Sensors

The sensor used in this study was the PurpleAir PA-II. The PA-II is marketed as PurpleAir's outdoor aerosol monitor, composed of a weatherproof plastic shell containing two Plantower PMS5003 sensors (labeled as "A" and "B" channels), an Adafruit model BME280 atmospheric sensor (temperature, RH, and pressure), and a wireless transmitter module to upload data via WiFi. The PMS5003 reports particulate matter (PM) mass concentrations ( $\mu\text{g}/\text{m}^3$ ) of all particles with an aerodynamic diameter smaller than 1  $\mu\text{m}$ , 2.5  $\mu\text{m}$ , and 10  $\mu\text{m}$ , as well as particle number concentrations ( $\text{dl}^{-1}$ ) of all particles larger than 0.3  $\mu\text{m}$ , 0.5  $\mu\text{m}$ , 1.0  $\mu\text{m}$ , 2.5  $\mu\text{m}$ , 5  $\mu\text{m}$ , and 10  $\mu\text{m}$  (Zhou and Zheng, 2016)).

PurpleAir reports mass concentrations from PA-IIs in three forms, referred to as CF1, ATM, and ALT. CF1 ("Correction Factor 1") is the "uncorrected" data from the Plantower. The CF1 data has been demonstrated to strongly correlate with collocated integrating nephelometer data (Ouimette et al., 2021). ATM or "Atmospheric Corrected" data uses a piece-wise function to attempt to account for overestimation. SI Figure S1 illustrates this function across the full dynamic range for data collected

in Delhi. Between 0 - 20  $\mu\text{g}/\text{m}^3$ , the CF1 and ATM data are 1:1, between 20 - 100  $\mu\text{g}/\text{m}^3$  the ATM to CF1 ratio transitions from 1:1 to approximately 0.66:1, and at greater than 100  $\mu\text{g}/\text{m}^3$  the ATM to CF1 ratio is stable at 0.66:1. Although it is reasonable to hypothesize the ATM data may better represent exposure ambient  $\text{PM}_{2.5}$  than the CF1 data, there is no transparent reasoning in the user manual for this design choice (Wallace et al., 2021; Zhou and Zheng, 2016). Finally, the ALT data represents a reconstruction of the  $\text{PM}_{2.5}$  data from the particle number data reported by the Plantower. Briefly, the ALT method adds all the particle counts from bins less than 2.5  $\mu\text{m}$ , and calculates the particle volume concentration assuming spherical particles. Particle volume concentration is then multiplied by unit density (1  $\text{g}/\text{cm}^3$ ) to estimate  $\text{PM}_{2.5}$  mass concentration. Wallace et al. (2021) and Wallace et al. (2020) used this data to develop calibration relationships, reporting the ALT data as more transparent than using the CF1 or ATM data. However, the particle number data is known not to reflect the actual ambient size distribution since the Plantower PMS5003 is not a particle sizing instrument, but rather reflects a modeled size distribution using assumptions for relationships between size bins that is not always accurate for atmospheric conditions (Ouimette et al., 2021; Hagan and Kroll, 2020; He et al., 2020; Kuula et al., 2020). SI Figure S1 shows the ALT to CF1 ratio is approximately 0.15:1. Although the CF1 and ATM data have dominated most calibration efforts (Malyan et al., 2023; Puttaswamy et al., 2022; Barkjohn et al., 2021; McFarlane et al., 2021; Magi et al., 2020; Malings et al., 2019), the usage of ALT data continues to propagate in peer-reviewed literature (Wallace and Zhao, 2023; Wallace and Ott, 2023). Therefore we use CF1, ATM, and ALT in our study to work towards harmonizing a calibration approach for PA-II in India.

## 2.2 Regulatory-grade Monitors

We compared our PurpleAir measurements against US EPA Federal Equivalent Method (FEM) certified continuous monitors. Our selected FEMs are MetOne BAM models 1020 and 1022, widely used devices (Hall and Gilliam, 2016) that use the beta wave attenuation technique to determine particle mass based on a sample deposited on a filter tape. FEM certification applies to 24-hour averaged data, while the BAMs can provide measurements at hourly or higher time resolution. We used the 1-hour block as our highest level of temporal resolution, similar to other low-cost sensor calibration studies using beta attenuation reference monitors in the US and India (Johnson et al., 2018; Magi et al., 2020; Sreekanth et al., 2022; Zheng et al., 2018).

At the Delhi site, we used the BAM-1020; data from this monitor are public and maintained by the US State Department's AirNow service (San Martini et al., 2015). The Hamirpur and Bangalore sites utilized BAM-1022s managed in collaboration with field teams from the Indo-Gangetic Plains Center for Air Research and Education and the Center for Study of Science, Technology, and Policy, who manually retrieved data at regular intervals. Staff at each site followed the manufacturer's recommended operation and maintenance, which resulted in downtime for each dataset.

## 2.3 Deployment Sites

Three separate long-term measurement efforts were conducted to evaluate the PA-II performance under different meteorological and aerosol composition regimes. Each campaign was scheduled to last approximately one year, enabling comparison of a range of mass loadings and the effect of season. We use the Indian Meteorological Department's (IMD) definition of four seasons: Winter (January, February), Pre-Monsoon (March, April, May), Monsoon (June, July, August, September), and Post-

115 Monsoon (October, November, December). (Dubey et al., 2021). A reference map of the collocation sites is presented in SI Fig. S2.

### 2.3.1 US Embassy, New Delhi, National Capital Territory of Delhi, India

The Indian National Capital Region, including the capital city of New Delhi (elevation about 230 m), is the second largest megacity in the world with a metro-area population of around 28.5 million people. It has also been called the most polluted  
120 megacity in the world, experiencing annual average  $PM_{2.5}$  concentrations exceeding  $120 \mu g/m^3$  (SI Fig. S3, Gani et al. (2019)). The National Capital Region along with the rest of North India experiences dynamic meteorology with cold wet winters, warm drier post-monsoons and pre-monsoons, and hot wet monsoons (SI Fig. S4).

Our measurement site was the US Embassy (28.5975 °N, 77.1878 °E) in the Chanakyapuri neighborhood of central New Delhi. The embassy is located within the city's spacious diplomatic enclave, which has abundant greenspace, relatively low  
125 traffic flows, and minimal local industrial emissions. We collocated 2 PA-II units with the embassy BAM from 2018 July - 2020 April. During the course of our campaign, Delhi experienced extreme  $PM_{2.5}$  concentrations during the post-monsoon agricultural burning seasons and characteristic winter inversion layers, with a relatively low-pollution monsoon season consistent with expected seasonal trends (Guttikunda and Gurjar, 2012).

### 2.3.2 Indo-Gangetic Plains Center for Atmospheric Research and Education, Hamirpur, Uttar Pradesh, India

We established a rural  $PM_{2.5}$  monitoring site in Hamirpur district, located within North India in India's most populous state, Uttar Pradesh (UP). Our monitoring site was established in partnership with the Indo-Gangetic Plains Center for Atmospheric Research and Education. This remote solar-powered rural monitoring site is situated on a rooftop (20 m above ground level) of a solitary building ((25.9552 °N, 80.1522 °E)) located about 800 m outside Ruri Para village in Hamirpur district, Uttar Pradesh. The immediate surroundings within 500 m of the site are a mixture of agricultural fields, ravines, and scrubland forests. The  
135 closest major town, Hamirpur (population about 35,000) is approximately 30 km away from the site, and the closest large city, Kanpur (population about 3 million) is 80 km away. Meteorological patterns are similar to Delhi (SI Fig. S5). We collocated three PA-II sensors with a BAM-1022 on the Indo-Gangetic Plains Center for Atmospheric Research and Education rooftop beginning in January 2020. Here, we report on data for the year from 2020 January to 2021 January.

Although campaign-median  $PM_{2.5}$  concentrations at the site (Table 1) are high in the global context, this site's remote  
140 location outside of both cities and villages means that concentrations do not reach the same peaks as in Delhi. However, there are still many local sources of aerosol air pollution in rural North India such as biomass burning for cooking and heating (Rooney et al., 2019). The Hamirpur dataset is additionally differentiated from the Delhi dataset in that most of the data was collected during the first year of the COVID-19 pandemic, which was observed to change patterns of emissions throughout India. (Patel et al., 2021; Singh et al., 2020).

### 145 2.3.3 Center for Study of Science, Technology and Policy, Bangalore, Karnataka, India

Bangalore, in South India, is the third largest city in India, with a population of 8.4 million, and the capital of Karnataka. South India experiences different meteorological conditions and considerably lower air pollution burdens than North India (Apte and Pant, 2019; Dubey et al., 2021) (SI Fig. S6, SI Fig. S7). Although continuous PM<sub>2.5</sub> regulatory monitors are sparse in Bangalore, the current network estimates a citywide annual average of 30  $\mu\text{g}/\text{m}^3$ . While the annual average is low in comparison to Delhi  
150 as well as the Indian National Ambient Air Quality Standard of 40  $\mu\text{g}/\text{m}^3$ , it exceeds the WHO annual guideline value of 5  $\mu\text{g}/\text{m}^3$  and hourly winter concentrations often exceed 50  $\mu\text{g}/\text{m}^3$ . Consequently, Bangalore has been designated for air quality improvement under the Indian National Clean Air Programme (Ganguly et al., 2020). In Bangalore, emissions are dominated by traffic and dust resuspension (Guttikunda et al., 2019). Compared to Delhi and Hamirpur, winters are milder, and the climate is more consistent year-round in Bangalore (SI Fig. S6). The winter and pre-monsoon seasons are distinguished from  
155 the monsoon and post-monsoon seasons primarily by RH and precipitation. Monsoon and post-monsoon are cloudy and rainy, with RH typically exceeding 70% all day, and can remain above 90% before sunrise. Winter and pre-monsoon RH are more moderate with hourly averages fluctuating between 40-80%.

Our collocation site was the Center for Study of Science, Technology and Policy office in northern Bangalore. We maintained a BAM-1022 on the rooftop of a 3-story office building (13.0485 °N, 77.5795 °E). Although the site is located near  
160 a highway (Outer Ring Road), the annual diurnal patterns matched the regional signature from the average of the regulatory monitors. Furthermore, the area surrounding the site is mostly office buildings, with some residential housing. There are no large industrial sites or obvious large point sources in the neighborhood, other than occasional small solid waste fires. It is likely the Bangalore BAM is thus mostly influenced by urban background and regional aerosol conditions. We set up 2 PA-II sensors from 2019 June – 2020 July, during which Bangalore experienced hourly spikes above 100  $\mu\text{g}/\text{m}^3$  during the festival  
165 of Diwali and dynamic changes in traffic patterns due to the COVID-19 pandemic and lockdowns.

## 2.4 Quality Assurance

### 2.4.1 PurpleAir PA-II PM<sub>2.5</sub>

Many light-scattering PM<sub>2.5</sub> sensors, including the PA-II, can report unrealistic measurements, lack accuracy (especially at high mass loadings), and are only recommended for operation within a specific range. To minimize these effects, we removed  
170 unreasonably small and large points (outside the range of 5 - 500  $\mu\text{g}/\text{m}^3$ ), hourly-averaged each individual Plantower unit, averaged across all units for a given site, removed imprecise points, and calibrated the resulting clean dataset. We conducted QA procedures separately for each sensor correction factor (CF1, ATM, ALT).

We removed all raw PM<sub>2.5</sub> data points outside of the range 5 – 500  $\mu\text{g}/\text{m}^3$  (Kelly et al., 2017; Magi et al., 2020; Zhou and Zheng, 2016). Analyses of PurpleAir data typically report the percent error between channels A and B for a given unit  
175 to remove imprecise points, treating them as joint measurements and all other nodes as independent (Barkjohn et al., 2021). However, at our collocation sites, there was always more than one PA-II, so we treated all Plantower sensors as replicate measurements and averaged them together as a single data point. For instance, if we had three PA-IIs at a site, we averaged

the six values together – two from each unit – to estimate a single data point. We established 80% completeness criteria (or 24 2-minute data points) for each hourly average, and at least 2 valid Plantower hourly averages for the resulting site PA data point. Imprecise site points were removed using the coefficient of variation (CV), the quotient of the standard deviation, and the mean of the collocated Plantower sensors for a given 2-min raw sample. CV values greater than 0.2 were removed, broadly consistent with approaches used by other studies (Badura et al., 2018; Crilley et al., 2018).

#### 2.4.2 PurpleAir PA-II Temperature and Relative Humidity

The Adafruit model BME280 is considered a reliable and accurate low-cost environmental sensor (Araújo et al., 2020). There are occasional sensor miscommunications with the microprocessor, leading to unrealistic values, which we filtered out by restricting RH to 0-100% and temperature to -10-50°C. We computed dew point temperature from the measured temperature and RH like Malings et al. (2019).

#### 2.4.3 MetOne BAM-1020, BAM-1022

The BAM instrument flags low-quality data with a specific code to (1) potentially remove them from analyses and (2) diagnose underlying issues, which can include power loss and pump errors. The BAM-1020 and BAM-1022's default concentration range is 3 - 1000  $\mu\text{g}/\text{m}^3$ . Unlike the PA-II, the hourly limit of detection of the BAM-1022 and BAM-1020 is well constrained to 2.4  $\mu\text{g}/\text{m}^3$  (Magi et al., 2020), considerably below typical concentrations in our dataset. Like other linear regression studies using MetOne BAMs models and Plantower nephelometers, we utilized an ordinary least squares approach (Barkjohn et al., 2021; Malings et al., 2019; McFarlane et al., 2021; Mehadi et al., 2020; Wallace et al., 2021; Zheng et al., 2018).

### 2.5 Calibration Regression

Since nephelometers and other optical-based sensors are known to provide biased measurements of  $\text{PM}_{2.5}$  measurements relative to reference grade instruments, in large part due to hygroscopic growth, calibration procedures attempt to account for bias due to RH, index of refraction, and mischaracterizing the particle size distribution. One approach is to leverage the environmental data (RH, temperature, etc.) from low-cost sensor nodes to develop the best-fitting model without imposing any a priori assumptions about aerosol growth or chemistry (Barkjohn et al., 2021; McFarlane et al., 2021; Malings et al., 2019; Wallace et al., 2021; Zheng et al., 2018). We label this approach as “data-driven.” From decades of work with optical instruments, corrections have been developed assigning non-linear growth terms as a function of RH and known  $\text{PM}_{2.5}$  chemical characteristics (Malings et al., 2019; Chakrabarti et al., 2004). In our work, we label this approach as “theory-driven” since it attempts to fuse the best-fitting function form from theory with the best-fitting regression coefficients. Although the theory-driven model should produce the most transferable models since theory should apply in all environments, the underlying data processing of the Plantower - a truncated nephelometer (Ouimette et al., 2021) - may result in a bias structure better explained by a linear RH correction than a non-linear correction for the dynamic range of RH under real-world conditions.

### 2.5.1 Data-Driven Model Selection

To ensure our work is easily reproducible within India, we relied only upon variables reported or calculable by the PA-II as independent variables: PM, RH, temperature, and dew point. For our PA-II PM<sub>2.5</sub> variable, we evaluated CF1, ATM, and ALT values. We evaluated all regression models using ordinary least squares with the BAM PM<sub>2.5</sub> as the dependent variable and our candidate parameters as independent variables. To iterate across all possible arrangements of predictors - including additive terms, interaction terms, as well as polynomial terms up to order 3 – we implemented Sequential Feature Selection (SFS) using the Python package scikit-learn 0.24.2. SFS uses a "greedy" approach to converge on the best-performing model for a user-defined number of parameters (Raschka and Mirjalili, 2019; James et al., 2013; Ferri et al., 1994). For example, if a user wanted a 2-parameter model from a set of 10 features, SFS would iteratively compare 90 models, the set of all possible 2-parameter feature permutations, using a robust regression metric (such as adjusted R<sup>2</sup> or Bayesian Information Criterion [BIC]). In our approach, we first use SFS to define the best-performing n-parameter model starting with all possible parameters (n=34). We then compare adjusted R<sup>2</sup> across best-performing n-parameter models to measure the impact of model complexity. If increasing parameters results in only marginal improvements ( $\Delta R^2 \approx 0.01$ ), then it is unnecessary to use those additional features. The overall most robust model, therefore, reflects both the best possible selection of features as well as feature parsimony.

### 2.5.2 Theory-Driven Model Selection

From  $\kappa$ -Köhler theory, we expect wet PM scattering to increase exponentially with increasing RH, resulting in strongly non-linear dynamics. Therefore, we applied a calibration function relying on empirically fitted coefficients from the training data, with a non-linear RH term to capture expected trends from theory. Studies have attempted applying a non-linear RH term for light scattering low-cost sensors, with results similar to or less accurate than an additive term (Chakrabarti et al., 2004; Malings et al., 2019; Tryner et al., 2020; Zheng et al., 2018). Given the difference in emission sources, size distribution, mass loadings, and meteorology, we decided to include a non-linear RH term using the following form, Eq. (1).

$$C = \frac{\alpha \times P}{1 + \beta \frac{RH^2}{1-RH}} \quad (1)$$

Where  $\alpha$  and  $\beta$  represent regression coefficients to be fitted via Non-linear Least Squares, P is the PurpleAir signal (ATM, CF1, or ALT), RH is the unitless relative humidity scaled from 0 to 1, and C represents the corrected PM<sub>2.5</sub>.

### 2.5.3 Cross-validation

To evaluate our calibration models, we sought to design an appropriate cross-validation scheme that would permit a balanced evaluation of model performance among all seasons. A simple test-train split would likely overrepresent seasons with more measurements. We thus performed a stratified k-fold cross-validation, in which each fold contains equal representation from each of the 4 seasons; we evaluated each model by leaving one-fold out in subsequent iterations.



#### 2.5.4 Temporal Sensitivity

As a point of contrast with the seasonally balanced calibration described above, we performed a data experiment to investigate the temporal stability of a hypothetical shorter-term calibration. This exercise was motivated by the common practice in many low-cost sensor deployments, of performing a short-term initial calibration, then deploying sensors in the field, and if the low-cost sensors are available, performing another short post-study collocation. Previously Levy Zamora et al. (2023) identified diminishing returns in improvements to calibration regressions after about 4 weeks of collocation in Baltimore, USA, if that period encapsulated a representative range of  $\text{PM}_{2.5}$  and RH conditions. Here we build on this work by seeking to identify which 4-week period is ideal at our sites in India since annual median  $\text{PM}_{2.5}$  concentrations at Delhi and Hamirpur sites are about 10× higher than Baltimore and reflect a different mixture of chemical composition and aerosol properties. To explore the potential bias from extrapolating a short-term calibration to a longer period, we fitted 4-week rolling ordinary least squares (ROLS) models with the features selected via SFS and compared the performance against all other 4-week periods during our yearlong data collection to understand the implications of short-term calibration for other studies.

#### 2.5.5 Performance Metrics

As a guiding principle, we selected for presentation those models which balanced parsimony with low error, low bias, and strong temporal consistency. We selected analytical methods and performance metrics to optimize these parameters and have designated these best-performing models as “robust.” Given the high concentrations and high variability within and between sites, we report the normalized RMSE (NRMSE), allowing a comparison of model performance across sites and time periods (Simon et al., 2012). Additionally, we used the coefficient of determination ( $R^2$ ) to evaluate model accuracy (Simon et al., 2012). For multivariate regression models, we used the adjusted  $R^2$  metric to account for spurious correlations with increasing numbers of independent variables. To penalize overfit and minimize the number of parameters, we used the Bayesian Information Criterion, a metric for parsimonious feature selection (James et al., 2013), when selecting between models during the SFS process. Finally, we assessed the mean bias error (MBE) as well as normalized mean bias error (NMBE) to characterize the average direction of error (Simon et al., 2012).

### 3 Results and Discussion

#### 3.1 Reference Instrument Data Summary and Quality Assurance

BAM and PA measurement summary statistics are summarized in Table 1 for each site, with time series plots in SI Fig. S8-S10. Overall, BAM monitors used at each site provided consistent performance despite challenging deployment circumstances due to intermittent power loss; extreme weather, including heavy rains; and a relatively broad range of mass concentrations.

The US State Department monitor in Delhi employs the US EPA’s data reduction process (San Martini et al., 2015; Vaughn, 2009), resulting in a loss of about 3% of data points, with a continuous gap from 2019 February 10 to 2019 March 18. For context, we compared this site’s time series with 39 other sites in Delhi’s regulatory network and found a  $R^2$  of 0.86 and a

mean difference from the regulatory network average of  $-8.41 \mu\text{g}/\text{m}^3$ , likely resulting from this monitor's location in one of the city's cleanest neighborhoods. The diurnal plot for the Delhi BAM in Fig. 1 reflects the roles of time-varying emissions and boundary layer dynamics with peaks during the morning traffic rush hour (7-10 AM), and extremes in the winter exceeding an average of  $200 \mu\text{g}/\text{m}^3$  during the night and early morning. During the monsoon, we observed a relatively low daily dynamic range of  $35\text{--}50 \mu\text{g}/\text{m}^3$ .

At both the site in Hamirpur and the site in Bangalore, we used the manufacturer's specified data flags to perform quality assurance, resulting in 6% and 11% data loss for the Hamirpur site and Bangalore site BAMs, respectively. Unlike Delhi, the Bangalore network is sparse ( $n = 40$  in Delhi versus  $n = 8$  in Bangalore), with relatively low data completeness from the official monitors. Diurnal plots in Fig. 1 show a morning peak, with maximum values typically at 8-9 AM for the collocation site BAM.

The closest regulatory monitor to the Hamirpur site is in Kanpur, more than 50 km away, too far for meaningful comparisons of local conditions. Figure 1 shows similar trends to the US Embassy site in Delhi, with a morning peak between 7 and 9 in the morning, extreme mass concentrations throughout the winter, and low dynamic range during the monsoon. There are no long continuous gaps from this monitor; however, power outages were more frequent in Hamirpur than the other two sites since it is a rural site, leading to significant data loss – about 14% of the total campaign hours, concentrated in the Pre-Monsoon.

### 3.2 PA-II Quality Assurance

We evaluated the unit-to-unit precision of the PA-II sensors by comparing the individual channels of all co-located Plantower sensors at each site. Because each PA-II contains two Plantower sensors, there were always a minimum of four Plantower sensors operating at each monitoring site. The PA-II  $\text{PM}_{2.5}$  channels were highly precise, with strong correlation ( $R^2 \geq 0.9$ ) both within nodes and between nodes across the mass concentration distribution, consistent with existing literature (Kelly et al., 2017; Levy Zamora et al., 2019; Sahu et al., 2020). Bland-Altman plots indicate high precision across all sites and units, with mean differences centered near  $0 \mu\text{g}/\text{m}^3$ , and most hourly points within  $\leq 20\%$  (SI Fig. S11-S13). The between-Plantower  $R^2$  for the CF1 data across all collocated PA-II sensors was between 0.94-0.99 for the Delhi site, 0.92-0.99 for the Bangalore site, and 0.95-0.99 for the Hamirpur site (SI Fig. S14). Disagreement was more pronounced at high concentrations ( $>100 \mu\text{g}/\text{m}^3$ ) at which  $R^2$  ranges at each site dropped to 0.90 – 0.95, 0.83 – 0.88, and 0.92 – 0.94 for Delhi, Hamirpur and Bangalore respectively. Similar intra-sensor correlations were found for the ATM and ALT data. Given the consistent between-sensor hourly precision across sites (NRMSE  $\leq 10\%$ ), we can confidently state we expect a random error of at most 10%.

Applying the detection limit thresholds removed 1% of the total Delhi dataset, and  $<1\%$  from the Hamirpur and Bangalore datasets. The CV test removed about 15% from each site. RH and temperature microcontroller errors were limited to about 4% of the total data in Delhi and Hamirpur and  $<1\%$  in Bangalore.

After removing the filtered data points, accounting for power losses, and applying the completeness criteria for 1-hr hourly averages, the site averaged PA data resulted in an average coverage of 47% ( $N=9260$  hours), 63% ( $N=5958$  hours), 86% ( $N=8567$  hours) for Delhi, Hamirpur, and Bangalore respectively across CFs. Finally, the reference dataset was synchronized with the PA dataset and the combined dataset coverage is 38% ( $N=7504$ ), 39% ( $N=3744$ ), and 75% ( $N=7473$ ) for Delhi,

Hamirpur, and Bangalore respectively. The smaller number of data points available for the Delhi and Hamirpur sites principally arose because of relatively more downtime of the BAM instruments at these two locations.

### 3.3 PurpleAir Data Summary

305 Across sites, the PA-II captured diurnal and seasonal trends with similar results to collocated BAMs, as evident in Fig. 1 and SI Fig. S15. However, inconsistent biases among season and location were also observed for all three  $PM_{2.5}$  channels (CF1, ATM, ALT), resulting in poor accuracy for the uncalibrated dataset. Although poor accuracy is unsurprising, our findings highlight the importance of dynamic emissions and meteorology across the Indian subcontinent as well as field performance at extreme mass concentrations.

310 In Delhi, the PA data (CF1) correctly identified winter and post-monsoon as the most polluted seasons, with a strong diurnal range peaking at 8-9 AM (Fig. 1). The PA also well characterized the Delhi monsoon, with a low diurnal range and a daily average less than  $60 \mu\text{g}/\text{m}^3$ . The uncalibrated low-cost sensor overestimates concentrations during the extremely polluted and humid post-monsoon and winter. There is notably more accurate performance during the dry and hot pre-monsoon, albeit with a tendency to underestimate mass concentrations relative to the reference at least half of the hours of the day. The PA units at  
315 Hamirpur follow a similar trend. Although both the Delhi and Hamirpur sites feature relatively low bias in the pre-monsoon period, they underestimate mass concentrations in this season, perhaps due to the influence of wind-blown mineral dust, as observed elsewhere in field and lab evaluations (Jaffe et al., 2023; Kuula et al., 2020; Levy Zamora et al., 2019; Sahu et al., 2020; Sayahi et al., 2019). While crustal material does not generally dominate  $PM_{2.5}$  mass, during dust storms the lower tail of the coarse mode aerosol can lead to substantially elevated  $PM_{2.5}$  concentrations in India.

320 Since Bangalore's meteorology exhibits comparatively low seasonality, and emissions are more strongly influenced by mobile sources rather than the more complex mixture in Delhi, low-cost sensor performance is different than in Delhi and Hamirpur. During the day (9 AM - 7 PM), accuracy is biased by more than +25% during the winter, pre-monsoon, and post-monsoon, with systemically lower bias including underestimates in the less polluted monsoon season (Fig. 1). Accuracy is lower during higher mass loadings at night and during early morning hours, with strong overestimates across seasons, peaking during the  
325 most polluted hour (7 - 8 AM).

### 3.4 Model Selection

#### 3.4.1 Data-Driven Model Fitting

The SFS results are summarized in Table 2 (with extended results in SI Tables S1-S3), where the four most relevant parameters are listed in order of decreasing importance for each CF and site. Across sites,  $R^2$  stabilized at 2-parameters (about 0.8 for  
330 Delhi, and about 0.9 for Hamirpur and Bangalore). For all sites, sensor estimated  $PM_{2.5}$  was generally selected as the single most relevant parameter for predicting concentrations measured by BAM followed by a variation of RH (i.e.,  $RH^2$ ,  $RH^3$ ). The form of the most robust Bangalore model is different from the Delhi and Hamirpur sites with an interaction term between temperature and ALT  $PM_{2.5}$  (rather than CF1  $PM_{2.5}$ ) selected as the most predictive  $PM_{2.5}$  data stream. Furthermore, the

Bangalore dataset ranked temperature and dew point as more relevant than the Delhi and Hamirpur datasets. Constraining Bangalore to the same top parameters as the Delhi and Hamirpur sites (CF1  $PM_{2.5}$  and RH) reveals only marginal differences ( $\Delta NRMSE \approx 2\%$ ) in performance from the most robust model selected by SFS (ALT  $PM_{2.5}$  and  $RH^3$ ). As such we choose to standardize our calibration across all sites with only CF1  $PM_{2.5}$  and RH as relevant parameters.

Regression coefficients of CF1  $PM_{2.5}$  data were positive values less than 1, indicating the CF1 data generally overestimate but are positively correlated with reference monitors. RH term coefficients at the Delhi and Hamirpur sites are negative, indicating increasing RH should negatively weigh the PA reading, consistent with the expected artifacts of hygroscopic growth in the atmosphere. The Bangalore dataset similarly assigns RH terms a negative weight. Temperature and dewpoint terms only imparted marginal improvements to calibration models ( $\Delta R^2 \approx 0.01$ , see SI Fig. S16), and it is not determinable if the models are deriving a spurious correlation or detecting underlying aerosol or instrument properties.

### 3.4.2 Theory-Driven Model Fitting

SI Table S4 summarizes the best-fitting model coefficients from the training dataset for each site and each CF. Across sites, the  $PM_{2.5}$  regression coefficient ( $\alpha$ ) does not vary substantially: about 14% for CF1. Hygroscopic growth regression coefficients ( $\beta$ ) vary greatly from site to site for CF1 even within the same region,  $\beta_{CF1}$  for Delhi is double that for Hamirpur, perhaps due to a higher abundance of hygroscopic species (Chen et al., 2022; Gani et al., 2019).

The lack of consistency in fit is reasonable, as the Plantower proprietary algorithm and underlying physical-optical design of nephelometers mean the sensor does not explicitly account for the underlying aerosol size distribution and composition. The resulting datasets are therefore somewhat divorced from the expected pattern based on  $\kappa$ -Köhler theory. The ALT dataset removes the proprietary ATM correction, as well as assumptions of particle density present in the CF1 data, resulting in more consistent  $\beta$  intra-regional values, though with less consistent  $\alpha$  values.

### 3.4.3 Model Evaluation

For the Delhi and Hamirpur sites, both located in North India, 2-parameter ATM and CF1 models yielded consistent improvements from 1-parameter models, as summarized in Fig. 3 for Delhi and Hamirpur respectively. The CF1 models were consistently more accurate than their ATM counterparts in Hamirpur, albeit by about 1% NRMSE and less than 1%  $R^2$ . Conversely, in Delhi, the ATM models systematically outperformed CF1 models by about 1% NRMSE and  $R^2$ . As evident in Fig. 1, Hamirpur experiences overall lower mass loadings than Delhi. Consequently, the absolute difference between the two signals due to the Plantower piecewise function (SI Fig. 1) above about  $20 \mu g/m^3$  is likely less important in Hamirpur than in Delhi, where mass loadings are consistently elevated.

The theory-driven hygroscopic growth correction consistently improved performance from the uncalibrated baseline data across sites by 12% for ATM and 60% for CF1, on average (Fig. 3). In Delhi and Hamirpur, the theory-driven model performs within about 2% of the 1-parameter models, and outperforms the 1-parameter ATM model in Hamirpur by 4.3%.

However, since the Plantower PMS5003 is a nephelometer, the signal should not necessarily follow the expected non-linear hygroscopic growth with increasing RH above 60% as expected from a size-resolved measurement technique (Crilley et al.,

2020; Hagan and Kroll, 2020). As a result, the 2-parameter CF1 models in Delhi and Hamirpur, with their additive RH terms, outperformed theory-driven by at least 3%. In Bangalore, the theory-driven model performance was comparable to the data-driven models (about 1% NRMSE, see Fig. 3). This contrast in performance between the two methods in North India is likely a result of the less seasonally variable meteorology and source mixtures in Bangalore, leading to less dynamic aerosol hygroscopicity.

Since CF1 data produces models as accurate as or more accurate than ATM models, has been validated in studies around the world, and does not feature the same non-linear behavior as the ATM channel, we recommend using CF1 for calibration in Delhi and Hamirpur. In Bangalore, the ALT data may be useful and warrants further study in similar environments, including across South India. From our results, the CF1 data is suitable for deployment in Bangalore and provides uniformity in calibration guidance. Additionally, the 2-parameter model (with RH as additive terms to  $PM_{2.5}$ ) follows previous studies (Barkjohn et al., 2021; McFarlane et al., 2021; Zheng et al., 2018) across continents and aerosol regimes.

In Barkjohn et al. (2021), the large sample size of PA-II across the continental United States was used to derive a similar calibration regression. In SI Tables S5-S6 we compare the NRMSE and MBE for our best CF1 model forms from the SFS procedure (up to 3 parameters), theory-driven CF1 model, and Barkjohn et al. (2021) model output. We have found from our seasonally-balanced test dataset that our models perform moderately better ( $\Delta$ NRMSE of about 5% across sites) than the EPA model, which is perhaps intuitive given the differences in PM composition and concentrations in India relative to the US. Furthermore, our site-specific models' MBEs are close to  $0 \mu\text{g}/\text{m}^3$ , while the Barkjohn et al. (2021) model systemically suppresses mass concentration estimates, with an MBE as high as  $22 \mu\text{g}/\text{m}^3$  in Delhi, compared to an MBE of  $-0.7 \mu\text{g}/\text{m}^3$  using the Delhi site-specific model or  $3.25 \mu\text{g}/\text{m}^3$  using the Hamirpur model on the Delhi test dataset. Overall, while the site-specific models we develop here clearly outperform the model of Barkjohn et al. (2021) for these three Indian sites, it is nonetheless striking that this US-developed calibration still performs quite well at these three Indian sites. Given these findings, we selected the following multi-season correction equations (Eq. (2-4)) for Delhi, Hamirpur, and Bangalore respectively. Although relatively simple, our calibration models greatly improve the reliability of low-cost sensor data across aerosol regimes. Figure 2 summarizes each model's bias in at each collocation site with seasonally, and diurnally segregated residuals. Across all sites, the monthly bias of the calibrated data is within  $\pm 25\%$ , in contrast to the uncalibrated data. Figure 3 summarizes model accuracy, with NRMSE improvements from uncalibrated data ranging between 5-20%. SI Figure S17 additionally explores the residual structure and demonstrates the value of the selected model forms at reducing bias due to RH, and mass loading factors. The calibrated residuals distributions demonstrate marked improvements across the full range of mass concentrations ( $5 - 500 \mu\text{g}/\text{m}^3$ ), unlike the raw residuals which show increasing uncertainty at high mass concentrations. The selected calibration equations reduce median bias to near 0% across sites, from median bias as high as 150% using the uncalibrated data at  $RH > 60\%$ . Figure 4 summarizes the performance of Eq. 2 - 4, highlighting that although performance is robust in the aggregate, seasonal and diurnal shifts in aerosol properties can shift performance and uncertainty bounds - therefore motivating further investigation into the role of calibration sensitivity to temporal factors.

$$C = 0.546 \times CF1 - 0.936 \times RH + 50.3 \text{ (Delhi)} \quad (2)$$

$$C = 0.496 \times CF1 - 0.296 \times RH + 22.0 \text{ (Hamirpur)} \quad (3)$$

$$C = 0.515 \times CF1 - 0.139 \times RH + 14.1 \text{ (Bangalore)} \quad (4)$$

### 3.5 Model Evaluation

#### 3.5.1 Temporal Sensitivity

405 To identify the stability of the model and its parameters, we computed the 4-week Rolling Ordinary Least Squares (ROLS) for each of our selected models and compared performance to all other 4-week moving ROLS models. Each model's NMBE across time is shown in Fig. 5, where the grey squares in the top panel indicate less than 50% data completeness. Additionally, the bottom panel of Fig. 5 tracks the distribution of the diagonal of the matrices present in the top panel of the figure. Across sites, the choice of calibration period greatly changes the performance of the regression throughout the rest of the dataset and  
 410 influences the selection of regression coefficients. SI Figure S18 additionally explores the absolute bias, demonstrating that Eq. (2-4) biases are centered near 0. SI Figure S19 illustrates the same analysis with NRMSE, showing that monthly ROLS model performance is generally stronger than the annual model within the training month, but rapidly deteriorates.

In Delhi, model performance and coefficient selection exhibit a seasonal pattern, with post-monsoon, and winter month models (Jan, Feb, March, Sept, Oct, Nov, Dec) performing well and selecting similar regression coefficients even across years  
 415 (SI Fig. S20). When evaluating model performance on data within the same season, NRMSE is typically below 30% and  $R^2$  is above 0.7. However, the post-monsoon and winter models perform poorly when evaluated on pre-monsoon data (March, Apr), with NRMSE exceeding 100% and  $R^2$  falling below 0.1. For even the best performing pre-monsoon models, NRMSE rises above 50% during the pre-monsoon period data and above 70% for other seasons. Monsoon models (May, June, July, August) also lack transferability to other seasons but perform well when evaluated on data from the same season (NRMSE < 30%).  
 420 Monsoon meteorological conditions contrast with other seasons – it is humid, windy, cloudy, hot, and frequently rains (SI Figs. S4-S6). These conditions result in lower emissions (i.e., less biomass burning for heating relative to winter), as well as act to suppress emissions (i.e., wet deposition) resulting in lower average seasonal mass concentrations in the Monsoon (SI Figs. S3 and S7). Consequently, models trained in the monsoon poorly translate to other seasons.

The Hamirpur ROLS results are like those of Delhi, but over a shorter period and with a more robust summer performance.  
 425 The pre-monsoon models fit the largest magnitude  $PM_{2.5}$  regression coefficient and fail to perform well (NRMSE > 50%) both within their own seasons' data and across other seasons' data. All other windows perform well (NRMSE  $\leq$  25%,  $R^2 \geq$  0.9) within their training window and across all other non-pre-monsoon test windows. The regression coefficients stabilize ( $\beta_{PM_{2.5}} \approx$  0.5,  $\beta_{RH} \approx$  -25), resulting in less seasonally variable model performance than in Delhi. Most likely Delhi's model's less robust performance across seasons relative to the Hamirpur model's performance is due to the broader diversity of sources

430 in Delhi, making it more difficult to constrain the uncertainty due to factors including hygroscopic growth and particle size distribution.

Bangalore and Hamirpur results are similar in that both models are relatively stable and transferable across seasons. Bangalore model performance degrades and features less season-to-season transferability in the monsoon season months (July and Aug) but features accurate performance (NRSME < 20%) for the other seasons. Regression coefficients in Bangalore are  
435 relatively consistent even, albeit with more spread during the pre-monsoon.

Although model results and calibration formulation differ across sites, the temporal sensitivity analysis reveals several key lessons. First, there is no “free lunch” or universal model. Rather, aerosol and meteorological regimes vary sharply by season, leading to underfit for annual models or overfit for seasonal models. Since annual models use data from across the distribution of aerosol compositions and size distributions, they generally perform within 5% of monthly models (SI Fig. S21). Outliers can  
440 be especially concerning at the physical limitations of nephelometers such as during Pre-Monsoon dust storms or the extremely humid Monsoon. Therefore, models trained within one single month-long period do not necessarily transfer well to the next month, even within the same season and model feature selection. Consequently, we recommend calibration procedures in India and other similar environments maintain a long-term collocation with at least one low-cost and reference pair after the initial collocation period in the region of interest.

### 445 **3.5.2 Spatial Transferability**

Due to proximity and similarities in climate and aerosol characteristics, and since data-driven models from Delhi and Hamirpur sites share the same parameters (CF1 and RH), we hypothesized that Delhi and Hamirpur models may be transferable. Figure 6 summarizes the relevant performance metrics with respect to spatial calibration transferability. The Hamirpur dataset performance weakened after applying the Delhi model ( $R^2$  decreased to 0.82, NRMSE increased to 39%) but still outperformed  
450 uncalibrated CF1 data. The Delhi dataset performance also weakened after applying the Hamirpur model ( $R^2$  decreased to 0.78, NRMSE increased to 35%), a relatively modest performance degradation. From this exercise, we understand that although  $PM_{2.5}$  is highly variable in Delhi and Hamirpur, there may be enough of a “fingerprint” in aerosol characteristics from the background site that a single calibration equation could provide an adequate performance improvement. However, a local calibration can provide performance improvements due to fine-scale  $PM_{2.5}$  variability unique to urban environments, especially  
455 for a megacity like Delhi.

Applying the Delhi and Hamirpur models to the Bangalore test dataset resulted in contrasting performance, with an NRMSE of 71% and 24% from the Delhi and Hamirpur models respectively. It is likely the largely regional aerosol from Hamirpur has enough overlap in speciation and mass concentration range with the Bangalore aerosol that the models are somewhat interchangeable. This hypothesis is additionally evidenced by the overlap in coefficients from the theory-driven hygroscopic  
460 growth equations. Clearly, the differences in the composition of the Delhi and Bangalore aerosols prevents exchange between models at these two sites, but with enough preserved from the regional contribution to support some support from the Hamirpur model to the Delhi data.

Some calibration efforts have sought a unified continental model for low-cost sensors by combining multiple reference and low-cost sensor pairs into one regression model (Barkjohn et al., 2021). Other studies have focused on interpolating between calibration sites to avoid washing out local effects, typically in a dense sensor network (Zheng et al., 2019). Our results show that although there are overarching similarities in model parameter selection, urban and rural environments are heterogeneous to the point of potentially barring a unified model. Additionally, seasonal variability within India necessitates at least monthly updates to model coefficients.

#### 4 Conclusions

We collocated low-cost sensors with reference grade PM<sub>2.5</sub> monitors in three environments in India, two urban (Delhi, and Bangalore) and one rural (Hamirpur) over the course of multiple seasons to characterize low-cost sensor performance across shifting emissions and meteorological regimes and develop calibration models. Internally, PA-II units demonstrated strong consistency, with low intra-sensor bias and high correlation. Relative to reference instruments, uncalibrated sensor performance varied diurnally and seasonally with shifts strongly associated with extreme mass concentrations, RH, and coarse mode particles. The low-cost sensor signal generally overestimated mass concentrations relative to the reference instruments, a trend observed in literature to be associated with hygroscopic growth (Jayaratne et al., 2018; Malings et al., 2019). We identified periods of low-cost sensor signal underestimation by a factor of 2 – 6× in the Pre-Monsoon in Delhi and Hamirpur, when supra-micron wind-blown dust particles are relatively abundant.

We demonstrated a relatively simple multilinear regression model using only the low-cost sensor PM<sub>2.5</sub> signal and low-cost sensor RH could produce results well correlated ( $R^2 \geq 0.8$ ) with the reference signal at each site. These site-specific models provide the basis for a computationally efficient, well-constrained (NRMSE  $\leq 25\%$ ), and scalable calibration approach for low-cost sensing in India, despite the non-stationary and diverse aerosol dynamics of the region. Furthermore, we showed our models can be transferred from site to site and still improve performance above the uncalibrated baseline, although a site-specific model generally has superior performance.

Our work also highlights a key caveat to low-cost sensor deployments and calibration in India, especially long-term deployment. Models trained at a site with only data from one season may perform more accurately within that season than a seasonally balanced model but are unreliable at other times of the year. Based on our analysis, we hypothesize that it is better to use a model developed at a background site such as Hamirpur to correct data from an urban environment such as Delhi, since the composition of PM in Hamirpur represents a good subset of the variability in Delhi. On the other hand, since there are PM species only found in some urban environments in India, using models from these industrial microenvironments are less likely to produce accurate results outside of the training location. Our results showed that seasonality is especially important given the contrast in meteorology and mass concentrations between the Pre-Monsoon and Monsoon seasons. Although a multilinear regression approach produces well-constrained results, these models are not transferrable among seasons. Therefore, we advise future deployments to continuously operate a collocation site with at least one reference and low-cost sensor pair to evaluate



495 calibration drift. Accounting for the temporal and spatial dynamics of aerosol characteristics will allow for the rapid scaling of  
low-cost sensors for communities in India to communities in need of transparent and accurate data.

*Data availability.* Hourly concentrations for BAM-1020/1022 PM<sub>2.5</sub> as well as all PurpleAir PM<sub>2.5</sub> channels (CF1, ATM and ALT), and PurpleAir meteorological data (Relative Humidity, Temperature, and Dew Point) used in this study are available via [doi.org/10.6078/D1RQ70](https://doi.org/10.6078/D1RQ70).

*Author contributions.* JSA, RKP, SV, MK, SG, SS, JG, and MJC designed the study. SV, HRM, MK, PA, AU, NB, SS, JG, and MJC carried  
500 out the data collection. MJC carried out the data processing and analyses. All co-authors contributed to the interpretation of results, writing,  
and reviewing the paper.

*Competing interests.* The authors declare that they have no conflict of interest.

*Acknowledgements.* We are grateful to Open Philanthropy and The University of Texas President's Award for Global Learning for their  
support. We are thankful to the US Embassy in New Delhi, the Center for Study of Science, Technology and Policy in Bangalore, and  
505 Indo-Gangetic Plains Center for Atmospheric Research and Education in Hamirpur for institutional support.

## References

- Apte, J. S. and Pant, P.: Toward cleaner air for a billion Indians, *Proceedings of the National Academy of Sciences*, 116, 10 614–10 616, <https://doi.org/10.1073/pnas.1905458116>, publisher: National Academy of Sciences Section: Commentary, 2019.
- Apte, J. S., Brauer, M., Cohen, A. J., Ezzati, M., and Pope, C. A.: Ambient PM<sub>2.5</sub> Reduces Global and Regional Life Expectancy, *Environmental Science & Technology Letters*, 5, 546–551, <https://doi.org/10.1021/acs.estlett.8b00360>, number: 9, 2018.
- Araújo, T., Silva, L., and Moreira, A.: Evaluation of Low-Cost Sensors for Weather and Carbon Dioxide Monitoring in Internet of Things Context, *IoT*, 1, 286–308, <https://doi.org/10.3390/iot1020017>, number: 2 Publisher: Multidisciplinary Digital Publishing Institute, 2020.
- Badura, M., Batog, P., Drzeniecka-Osiadacz, A., and Modzel, P.: Evaluation of Low-Cost Sensors for Ambient PM<sub>2.5</sub> Monitoring, *Journal of Sensors*, 2018, e5096 540, <https://doi.org/10.1155/2018/5096540>, publisher: Hindawi, 2018.
- 515 Bai, L., Huang, L., Wang, Z., Ying, Q., Zheng, J., Shi, X., and Hu, J.: Long-term Field Evaluation of Low-cost Particulate Matter Sensors in Nanjing, *Aerosol and Air Quality Research*, 20, 242–253, <https://doi.org/10.4209/aaqr.2018.11.0424>, number: 2 Publisher: Taiwan Association for Aerosol Research, 2020.
- Barkjohn, K. K., Gantt, B., and Clements, A. L.: Development and application of a United States-wide correction for PM<sub>2.5</sub> data collected with the PurpleAir sensor, *Atmospheric Measurement Techniques*, 14, 4617–4637, <https://doi.org/10.5194/amt-14-4617-2021>, publisher: 520 Copernicus GmbH, 2021.
- Brauer, M., Guttikunda, S. K., K a, N., Dey, S., Tripathi, S. N., Weagle, C., and Martin, R. V.: Examination of monitoring approaches for ambient air pollution: A case study for India, *Atmospheric Environment*, 216, 116 940, <https://doi.org/10.1016/j.atmosenv.2019.116940>, 2019.
- Chakrabarti, B., Fine, P. M., Delfino, R., and Sioutas, C.: Performance evaluation of the active-flow personal DataRAM PM<sub>2.5</sub> mass monitor (Thermo Anderson pDR-1200) designed for continuous personal exposure measurements, *Atmospheric Environment*, 38, 3329–3340, <https://doi.org/10.1016/j.atmosenv.2004.03.007>, number: 20, 2004.
- 525 Chen, Y., Wang, Y., Nenes, A., Wild, O., Song, S., Hu, D., Liu, D., He, J., Hildebrandt Ruiz, L., Apte, J. S., Gunthe, S. S., and Liu, P.: Ammonium Chloride Associated Aerosol Liquid Water Enhances Haze in Delhi, India, *Environmental Science & Technology*, 56, 7163–7173, <https://doi.org/10.1021/acs.est.2c00650>, publisher: American Chemical Society, 2022.
- 530 Collaborators, I. S.-L. D. B. I. A. P.: Health and economic impact of air pollution in the states of India: the Global Burden of Disease Study 2019, *The Lancet Planetary Health*, 5, e25–e38, [https://doi.org/10.1016/S2542-5196\(20\)30298-9](https://doi.org/10.1016/S2542-5196(20)30298-9), 2021.
- Crilley, L. R., Shaw, M., Pound, R., Kramer, L. J., Price, R., Young, S., Lewis, A. C., and Pope, F. D.: Evaluation of a low-cost optical particle counter (Alphasense OPC-N2) for ambient air monitoring, *Atmospheric Measurement Techniques*, 11, 709–720, <https://doi.org/https://doi.org/10.5194/amt-11-709-2018>, number: 2 Publisher: Copernicus GmbH, 2018.
- 535 Crilley, L. R., Singh, A., Kramer, L. J., Shaw, M. D., Alam, M. S., Apte, J. S., Bloss, W. J., Hildebrandt Ruiz, L., Fu, P., Fu, W., Gani, S., Gatari, M., Ilyinskaya, E., Lewis, A. C., Ng'ang'a, D., Sun, Y., Whitty, R. C. W., Yue, S., Young, S., and Pope, F. D.: Effect of aerosol composition on the performance of low-cost optical particle counter correction factors, *Atmospheric Measurement Techniques*, pp. 1181–1193, <https://doi.org/10.5194/amt-13-1181-2020>, num Pages: 13 Publisher: York, 2020.
- 540 Dey, S., Purohit, B., Balyan, P., Dixit, K., Bali, K., Kumar, A., Imam, F., Chowdhury, S., Ganguly, D., Gargava, P., and Shukla, V. K.: A Satellite-Based High-Resolution (1-km) Ambient PM<sub>2.5</sub> Database for India over Two Decades (2000–2019): Applications for Air Quality Management, *Remote Sensing*, 12, 3872, <https://doi.org/10.3390/rs12233872>, number: 23 Publisher: Multidisciplinary Digital Publishing Institute, 2020.

- 545 Diseases, G. . and Collaborators, I.: Global burden of 369 diseases and injuries in 204 countries and territories, 1990–2019: a systematic analysis for the Global Burden of Disease Study 2019, *The Lancet*, 396, 1204–1222, [https://doi.org/10.1016/S0140-6736\(20\)30925-9](https://doi.org/10.1016/S0140-6736(20)30925-9), 2020.
- Dubey, A. K., Kumar, P., Saharwardi, M. S., and Javed, A.: Understanding the hot season dynamics and variability across India, *Weather and Climate Extremes*, 32, 100317, <https://doi.org/10.1016/j.wace.2021.100317>, 2021.
- 550 Ferri, F. J., Pudil, P., Hatef, M., and Kittler, J.: Comparative study of techniques for large-scale feature selection, in: *Machine Intelligence and Pattern Recognition*, edited by Gelsema, E. S. and Kanal, L. S., vol. 16 of *Pattern Recognition in Practice IV*, pp. 403–413, North-Holland, <https://doi.org/10.1016/B978-0-444-81892-8.50040-7>, 1994.
- Ganguly, T., Selvaraj, K. L., and Guttikunda, S. K.: National Clean Air Programme (NCAP) for Indian cities: Review and outlook of clean air action plans, *Atmospheric Environment: X*, 8, 100096, <https://doi.org/10.1016/j.aeaoa.2020.100096>, 2020.
- 555 Gani, S., Bhandari, S., Seraj, S., Wang, D. S., Patel, K., Soni, P., Arub, Z., Habib, G., Ruiz, L. H., and Apte, J. S.: Submicron aerosol composition in the world’s most polluted megacity: the Delhi Aerosol Supersite study, *Atmospheric Chemistry and Physics*; Katlenburg-Lindau, 19, 6843–6859, <https://doi.org/http://dx.doi.org.ezproxy.lib.utexas.edu/10.5194/acp-19-6843-2019>, number: 10, 2019.
- Gupta, L., Dev, R., Zaidi, K., Sunder Raman, R., Habib, G., and Ghosh, B.: Assessment of PM10 and PM2.5 over Ghaziabad, an industrial city in the Indo-Gangetic Plain: spatio-temporal variability and associated health effects, *Environmental Monitoring and Assessment*, 193, 735, <https://doi.org/10.1007/s10661-021-09411-5>, 2021.
- 560 Guttikunda, S. K. and Gurjar, B. R.: Role of meteorology in seasonality of air pollution in megacity Delhi, India, *Environmental Monitoring and Assessment*, 184, 3199–3211, <https://doi.org/10.1007/s10661-011-2182-8>, 2012.
- Guttikunda, S. K., Nishadh, K. A., Gota, S., Singh, P., Chanda, A., Jawahar, P., and Asundi, J.: Air quality, emissions, and source contributions analysis for the Greater Bengaluru region of India, *Atmospheric Pollution Research*, 10, 941–953, <https://doi.org/10.1016/j.apr.2019.01.002>, number: 3, 2019.
- 565 Hagan, D. H. and Kroll, J. H.: Assessing the accuracy of low-cost optical particle sensors using a physics-based approach, preprint, *Aerosols/Laboratory Measurement/Data Processing and Information Retrieval*, <https://doi.org/10.5194/amt-2020-188>, 2020.
- Hagler, G. S. W., Williams, R., Papapostolou, V., and Polidori, A.: Air Quality Sensors and Data Adjustment Algorithms: When Is It No Longer a Measurement?, *Environmental Science & Technology*, 52, 5530–5531, <https://doi.org/10.1021/acs.est.8b01826>, number: 10 Publisher: American Chemical Society, 2018.
- 570 Hall, E. and Gilliam, J.: Reference and Equivalent Methods Used to Measure National Ambient Air Quality Standards (NAAQS) Criteria Air Pollutants - Volume I, <https://doi.org/10.13140/RG.2.1.2423.2563>, 2016.
- Hammer, M. S., van Donkelaar, A., Li, C., Lyapustin, A., Sayer, A. M., Hsu, N. C., Levy, R. C., Garay, M. J., Kalashnikova, O. V., Kahn, R. A., Brauer, M., Apte, J. S., Henze, D. K., Zhang, L., Zhang, Q., Ford, B., Pierce, J. R., and Martin, R. V.: Global Estimates and Long-Term Trends of Fine Particulate Matter Concentrations (1998–2018), *Environmental Science & Technology*, 54, 7879–7890, <https://doi.org/10.1021/acs.est.0c01764>, number: 13 Publisher: American Chemical Society, 2020.
- 575 He, M., Kuerbanjiang, N., and Dhaniyala, S.: Performance characteristics of the low-cost Plantower PMS optical sensor, *Aerosol Science and Technology*, 54, 232–241, <https://doi.org/10.1080/02786826.2019.1696015>, number: 2 Publisher: Taylor & Francis \_eprint: <https://doi.org/10.1080/02786826.2019.1696015>, 2020.
- 580 Jaffe, D. A., Miller, C., Thompson, K., Finley, B., Nelson, M., Ouimette, J., and Andrews, E.: An evaluation of the U.S. EPA’s correction equation for PurpleAir sensor data in smoke, dust, and wintertime urban pollution events, *Atmospheric Measurement Techniques*, 16, 1311–1322, <https://doi.org/10.5194/amt-16-1311-2023>, publisher: Copernicus GmbH, 2023.

- James, G., Witten, D., Hastie, T., and Tibshirani, R.: An introduction to statistical learning, vol. 112, Springer, 2013.
- Jayaratne, R., Liu, X., Thai, P., Dunbabin, M., and Morawska, L.: The influence of humidity on the performance of a low-cost air particle mass sensor and the effect of atmospheric fog, *Atmospheric Measurement Techniques*, 11, 4883–4890, <https://doi.org/https://doi.org/10.5194/amt-11-4883-2018>, number: 8 Publisher: Copernicus GmbH, 2018.
- 585 Jha, S. K., Kumar, M., Arora, V., Tripathi, S. N., Motghare, V. M., Shingare, A. A., Rajput, K. A., and Kamble, S.: Domain Adaptation-Based Deep Calibration of Low-Cost PM<sub>2.5</sub> Sensors, *IEEE Sensors Journal*, 21, 25 941–25 949, <https://doi.org/10.1109/JSEN.2021.3118454>, conference Name: IEEE Sensors Journal, 2021.
- Johnson, K. K., Bergin, M. H., Russell, A. G., and Hagler, G. S.: Field Test of Several Low-Cost Particulate Matter Sensors in High and Low Concentration Urban Environments, *Aerosol and air quality research*, 18, 565–578, <https://doi.org/10.4209/aaqr.2017.10.0418>, number: 3, 2018.
- 590 Kelly, K. E., Whitaker, J., Petty, A., Widmer, C., Dybwad, A., Sleeth, D., Martin, R., and Butterfield, A.: Ambient and laboratory evaluation of a low-cost particulate matter sensor, *Environmental Pollution*, 221, 491–500, <https://doi.org/10.1016/j.envpol.2016.12.039>, 2017.
- Krishna, B., Mandal, S., Madhipatla, K., Reddy, K., Prabhakaran, D., and Schwartz, J.: Daily nonaccidental mortality associated with short-Term PM<sub>2.5</sub> exposures in Delhi, India, *Environmental Epidemiology*, <https://doi.org/10.1097/EE9.000000000000167>, 2021.
- 595 Kuula, J., Mäkelä, T., Aurela, M., Teinilä, K., Varjonen, S., González, O., and Timonen, H.: Laboratory evaluation of particle-size selectivity of optical low-cost particulate matter sensors, *Atmospheric Measurement Techniques*, 13, 2413–2423, <https://doi.org/https://doi.org/10.5194/amt-13-2413-2020>, number: 5 Publisher: Copernicus GmbH, 2020.
- Lepeule, J., Laden, F., Dockery, D., and Schwartz, J.: Chronic Exposure to Fine Particles and Mortality: An Extended Follow-up of the Harvard Six Cities Study from 1974 to 2009, *Environmental Health Perspectives*, 120, 965–970, <http://www.jstor.org/stable/41548777>, number: 7, 2012.
- 600 Levy Zamora, M., Xiong, F., Gentner, D., Kerkez, B., Kohrman-Glaser, J., and Koehler, K.: Field and Laboratory Evaluations of the Low-Cost Plantower Particulate Matter Sensor, *Environmental Science & Technology*, 53, 838–849, <https://doi.org/10.1021/acs.est.8b05174>, number: 2, 2019.
- Levy Zamora, M., Buehler, C., Datta, A., Gentner, D. R., and Koehler, K.: Identifying optimal co-location calibration periods for low-cost sensors, *Atmospheric Measurement Techniques*, 16, 169–179, <https://doi.org/10.5194/amt-16-169-2023>, publisher: Copernicus GmbH, 2023.
- 605 Magi, B. I., Cupini, C., Francis, J., Green, M., and Hauser, C.: Evaluation of PM<sub>2.5</sub> measured in an urban setting using a low-cost optical particle counter and a Federal Equivalent Method Beta Attenuation Monitor, *Aerosol Science and Technology*, 54, 147–159, <https://doi.org/10.1080/02786826.2019.1619915>, number: 2, 2020.
- 610 Malings, C., Tanzer, R., Hauryliuk, A., Saha, P. K., Robinson, A. L., Presto, A. A., and Subramanian, R.: Fine particle mass monitoring with low-cost sensors: Corrections and long-term performance evaluation, *Aerosol Science and Technology*, 0, 1–15, <https://doi.org/10.1080/02786826.2019.1623863>, number: 0, 2019.
- Malyan, V., Kumar, V., and Sahu, M.: Significance of sources and size distribution on calibration of low-cost particle sensors: Evidence from a field sampling campaign, *Journal of Aerosol Science*, 168, 106 114, <https://doi.org/10.1016/j.jaerosci.2022.106114>, 2023.
- 615 Martin, R. V., Brauer, M., van Donkelaar, A., Shaddick, G., Narain, U., and Dey, S.: No one knows which city has the highest concentration of fine particulate matter, *Atmospheric Environment: X*, 3, 100 040, <https://doi.org/10.1016/j.aeaoa.2019.100040>, 2019.
- McFarlane, C., Isevlambire, P. K., Lumbuenamo, R. S., Ndinga, A. M. E., Dhammapala, R., Jin, X., McNeill, V. F., Malings, C., Subramanian, R., and Westervelt, D. M.: First Measurements of Ambient PM<sub>2.5</sub> in Kinshasa, Democratic Republic of Congo

- and Brazzaville, Republic of Congo Using Field-calibrated Low-cost Sensors, *Aerosol and Air Quality Research*, 21, 200619, <https://doi.org/10.4209/aaqr.200619>, publisher: Taiwan Association for Aerosol Research, 2021.
- 620 Mehadi, A., Moosmüller, H., Campbell, D. E., Ham, W., Schweizer, D., Tarnay, L., and Hunter, J.: Laboratory and field evaluation of real-time and near real-time PM<sub>2.5</sub> smoke monitors, *Journal of the Air & Waste Management Association*, 70, 158–179, <https://doi.org/10.1080/10962247.2019.1654036>, number: 2 Publisher: Taylor & Francis \_eprint: <https://doi.org/10.1080/10962247.2019.1654036>, 2020.
- 625 Ouimette, J. R., Malm, W. C., Schichtel, B. A., Sheridan, P. J., Andrews, E., Ogren, J. A., and Arnott, W. P.: Evaluating the PurpleAir monitor as an aerosol light scattering instrument, *Atmospheric Measurement Techniques Discussions*, pp. 1–35, <https://doi.org/10.5194/amt-2021-170>, publisher: Copernicus GmbH, 2021.
- Patel, K., Campmier, M. J., Bhandari, S., Baig, N., Gani, S., Habib, G., Apte, J. S., and Hildebrandt Ruiz, L.: Persistence of Primary and Secondary Pollutants in Delhi: Concentrations and Composition from 2017 through the COVID Pandemic, *Environmental Science & Technology Letters*, 8, 492–497, <https://doi.org/10.1021/acs.estlett.1c00211>, publisher: American Chemical Society, 2021.
- 630 Puttaswamy, N., Sreekanth, V., Pillarisetti, A., Upadhy, A. R., Saidam, S., Veerappan, B., Mukhopadhyay, K., Sambandam, S., Sutaria, R., and Balakrishnan, K.: Indoor and Ambient Air Pollution in Chennai, India during COVID-19 Lockdown: An Affordable Sensors Study, *Aerosol and Air Quality Research*, 22, 210 170, <https://doi.org/10.4209/aaqr.210170>, publisher: Taiwan Association for Aerosol Research, 2022.
- 635 Ramachandra, T. V., Sellers, J., Bharath, H. A., and Setturu, B.: Micro level analyses of environmentally disastrous urbanization in Bangalore, *Environmental Monitoring and Assessment*, 191, 787, <https://doi.org/10.1007/s10661-019-7693-8>, number: 3, 2020.
- Raschka, S. and Mirjalili, V.: *Python machine learning: Machine learning and deep learning with Python, scikit-learn, and TensorFlow 2*, Packt Publishing Ltd, 2019.
- Rooney, B., Zhao, R., Wang, Y., Bates, K. H., Pillarisetti, A., Sharma, S., Kundu, S., Bond, T. C., Lam, N. L., Ozaltun, B., Xu, L., Goel, V., Fleming, L. T., Weltman, R., Meinardi, S., Blake, D. R., Nizkorodov, S. A., Edwards, R. D., Yadav, A., Arora, N. K., Smith, K. R., and Seinfeld, J. H.: Impacts of household sources on air pollution at village and regional scales in India, *Atmospheric Chemistry and Physics*, 19, 7719–7742, <https://doi.org/10.5194/acp-19-7719-2019>, publisher: Copernicus GmbH, 2019.
- 640 Sahu, R., Dixit, K. K., Mishra, S., Kumar, P., Shukla, A. K., Sutaria, R., Tiwari, S., and Tripathi, S. N.: Validation of Low-Cost Sensors in Measuring Real-Time PM<sub>10</sub> Concentrations at Two Sites in Delhi National Capital Region, *Sensors*, 20, 1347, <https://doi.org/10.3390/s20051347>, number: 5 Publisher: Multidisciplinary Digital Publishing Institute, 2020.
- San Martini, F. M., Hasenkopf, C. A., and Roberts, D. C.: Statistical analysis of PM<sub>2.5</sub> observations from diplomatic facilities in China, *Atmospheric Environment*, 110, 174–185, <https://doi.org/10.1016/j.atmosenv.2015.03.060>, 2015.
- Sayahi, T., Butterfield, A., and Kelly, K. E.: Long-term field evaluation of the Plantower PMS low-cost particulate matter sensors, *Environmental Pollution*, 245, 932–940, <https://doi.org/10.1016/j.envpol.2018.11.065>, 2019.
- 650 Simon, H., Baker, K. R., and Phillips, S.: Compilation and interpretation of photochemical model performance statistics published between 2006 and 2012, *Atmospheric Environment*, 61, 124–139, <https://doi.org/10.1016/j.atmosenv.2012.07.012>, 2012.
- Singh, V., Singh, S., Biswal, A., Kesarkar, A. P., Mor, S., and Ravindra, K.: Diurnal and temporal changes in air pollution during COVID-19 strict lockdown over different regions of India, *Environmental Pollution*, 266, 115 368, <https://doi.org/10.1016/j.envpol.2020.115368>, 2020.
- 655 Sreekanth, V., R., A. B., Kulkarni, P., Puttaswamy, N., Prabhu, V., Agrawal, P., Upadhy, A. R., Rao, S., Sutaria, R., Mor, S., Dey, S., Khaiwal, R., Balakrishnan, K., Tripathi, S. N., and Singh, P.: Inter- versus Intracity Variations in the Performance

- and Calibration of Low-Cost PM<sub>2.5</sub> Sensors: A Multicity Assessment in India, *ACS Earth and Space Chemistry*, 6, 3007–3016, <https://doi.org/10.1021/acsearthspacechem.2c00257>, publisher: American Chemical Society, 2022.
- 660 Tryner, J., L'Orange, C., Mehaffy, J., Miller-Lionberg, D., Hofstetter, J. C., Wilson, A., and Volckens, J.: Laboratory evaluation of low-cost PurpleAir PM monitors and in-field correction using co-located portable filter samplers, *Atmospheric Environment*, 220, 117 067, <https://doi.org/10.1016/j.atmosenv.2019.117067>, 2020.
- Vaughn, D. L.: Standard Operating Procedure for the Continuous Measurement of Particulate Matter, [https://www3.epa.gov/ttnamti1/files/ambient/pm25/sop\\_project/905505\\_BAM\\_SOP\\_Draft\\_Final\\_Oct09.pdf](https://www3.epa.gov/ttnamti1/files/ambient/pm25/sop_project/905505_BAM_SOP_Draft_Final_Oct09.pdf), 2009.
- 665 Wallace, L. and Ott, W.: Long-Term Indoor-Outdoor PM<sub>2.5</sub> Measurements Using PurpleAir Sensors: An Improved Method of Calculating Indoor-Generated and Outdoor-Infiltrated Contributions to Potential Indoor Exposure, *Sensors*, 23, 1160, <https://doi.org/10.3390/s23031160>, number: 3 Publisher: Multidisciplinary Digital Publishing Institute, 2023.
- Wallace, L. and Zhao, T.: Spatial Variation of PM<sub>2.5</sub> Indoors and Outdoors: Results from 261 Regulatory Monitors Compared to 14,000 Low-Cost Monitors in Three Western States over 4.7 Years, *Sensors*, 23, 4387, <https://doi.org/10.3390/s23094387>, number: 9 Publisher: Multidisciplinary Digital Publishing Institute, 2023.
- 670 Wallace, L., Ott, W., Zhao, T., Cheng, K.-C., and Hildemann, L.: Secondhand exposure from vaping marijuana: Concentrations, emissions, and exposures determined using both research-grade and low-cost monitors, *Atmospheric Environment: X*, 8, 100 093, <https://doi.org/10.1016/j.aeaoa.2020.100093>, 2020.
- Wallace, L., Bi, J., Ott, W. R., Sarnat, J., and Liu, Y.: Calibration of low-cost PurpleAir outdoor monitors using an improved method of calculating PM<sub>2.5</sub>, *Atmospheric Environment*, 256, 118 432, <https://doi.org/10.1016/j.atmosenv.2021.118432>, 2021.
- 675 Zheng, T., Bergin, M. H., Johnson, K. K., Tripathi, S. N., Shirodkar, S., Landis, M. S., Sutaria, R., and Carlson, D. E.: Field evaluation of low-cost particulate matter sensors in high- and low-concentration environments, *Atmospheric Measurement Techniques*, 11, 4823–4846, <https://doi.org/https://doi.org/10.5194/amt-11-4823-2018>, number: 8 Publisher: Copernicus GmbH, 2018.
- Zheng, T., Bergin, M. H., Sutaria, R., Tripathi, S. N., Caldow, R., and Carlson, D. E.: Gaussian Process regression model for dynamically calibrating a wireless low-cost particulate matter sensor network in Delhi, preprint, *Aerosols/In Situ Measurement/Data Processing and Information Retrieval*, <https://doi.org/10.5194/amt-2019-55>, 2019.
- 680 Zhou, Y. and Zheng, H.: PMS5003 Series Data Manual, [http://www.aqmd.gov/docs/default-source/qa-spec/resources-page/plantower-pms5003-manual\\_v2-3.pdf?sfvrsn=2](http://www.aqmd.gov/docs/default-source/qa-spec/resources-page/plantower-pms5003-manual_v2-3.pdf?sfvrsn=2), 2016.
- Zou, Y., Clark, J. D., and May, A. A.: Laboratory evaluation of the effects of particle size and composition on the performance of integrated devices containing Plantower particle sensors, *Aerosol Science and Technology*, 0, 1–13, <https://doi.org/10.1080/02786826.2021.1905148>, publisher: Taylor & Francis \_eprint: <https://doi.org/10.1080/02786826.2021.1905148>, 2021.
- 685

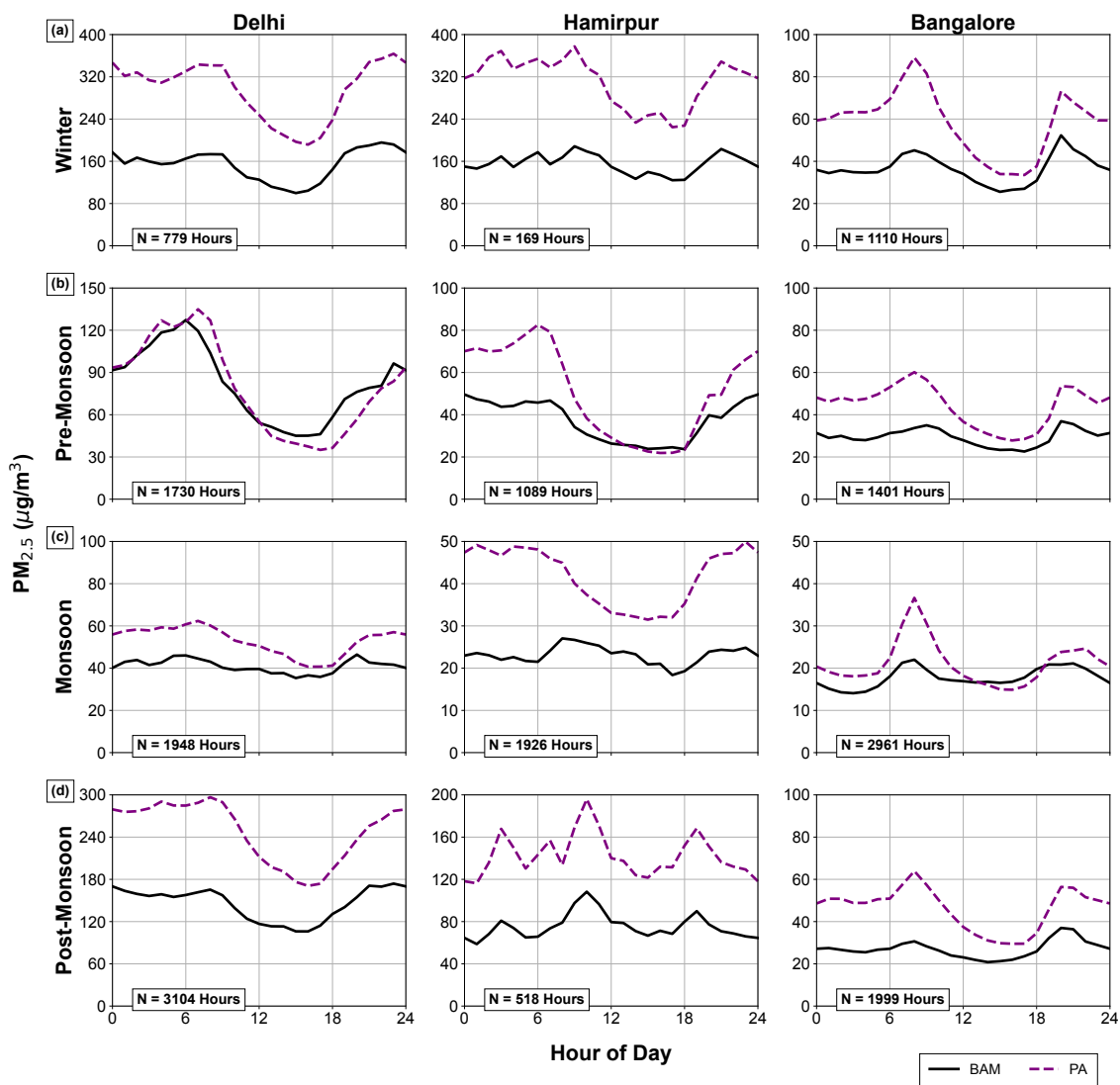


**Figure 1.** Diurnal profiles of mean hourly seasonal BAM (reference) and uncorrected PA  $PM_{2.5}$  signals for Delhi, Hamirpur, and Bangalore using the CF1 channel. The number of valid hourly averages (quality assured according to methods outlined in Sect. 2.4 and summarized in Sects. 3.1 - 3.3) in each dataset is presented in the bottom left of each subplot. Winter (January, February), Pre-Monsoon (March, April, May), Monsoon (June, July, August, September), and Post-Monsoon (October, November, December). No single hour of day represents more than about 7% to the total dataset shown in the bottom left corner of each plot.

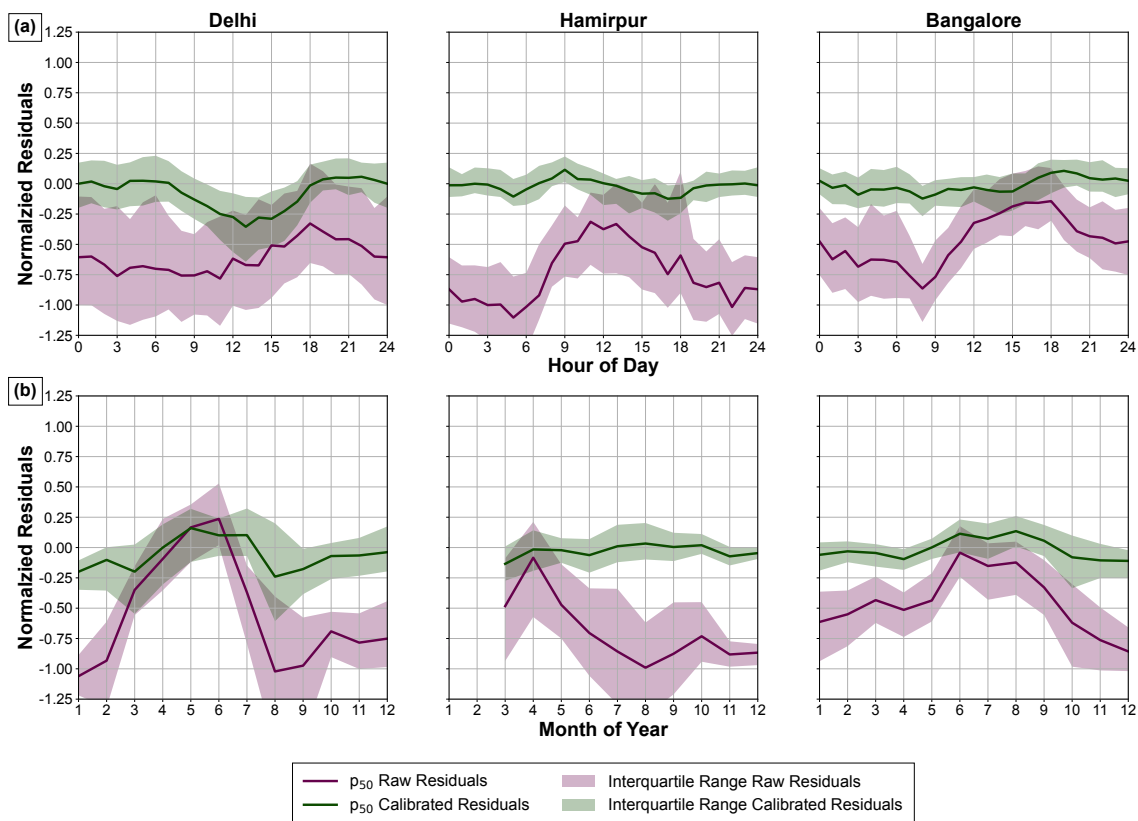


**Figure 2.** Normalized Residual distributions for the uncalibrated PurpleAir data (CF1) and the Calibration Models for each site. Bold lines represent the median ( $p_{50}$ ) of the distribution, while the shaded area represents the interquartile range ( $p_{75} - p_{25}$ ). Panel (a) shows the diurnal distribution, while panel (b) shows the normalized residual distribution binned by month. Compared to the residual distribution for uncalibrated (raw) data, the calibration effectively eliminates most seasonal and diurnal biases.



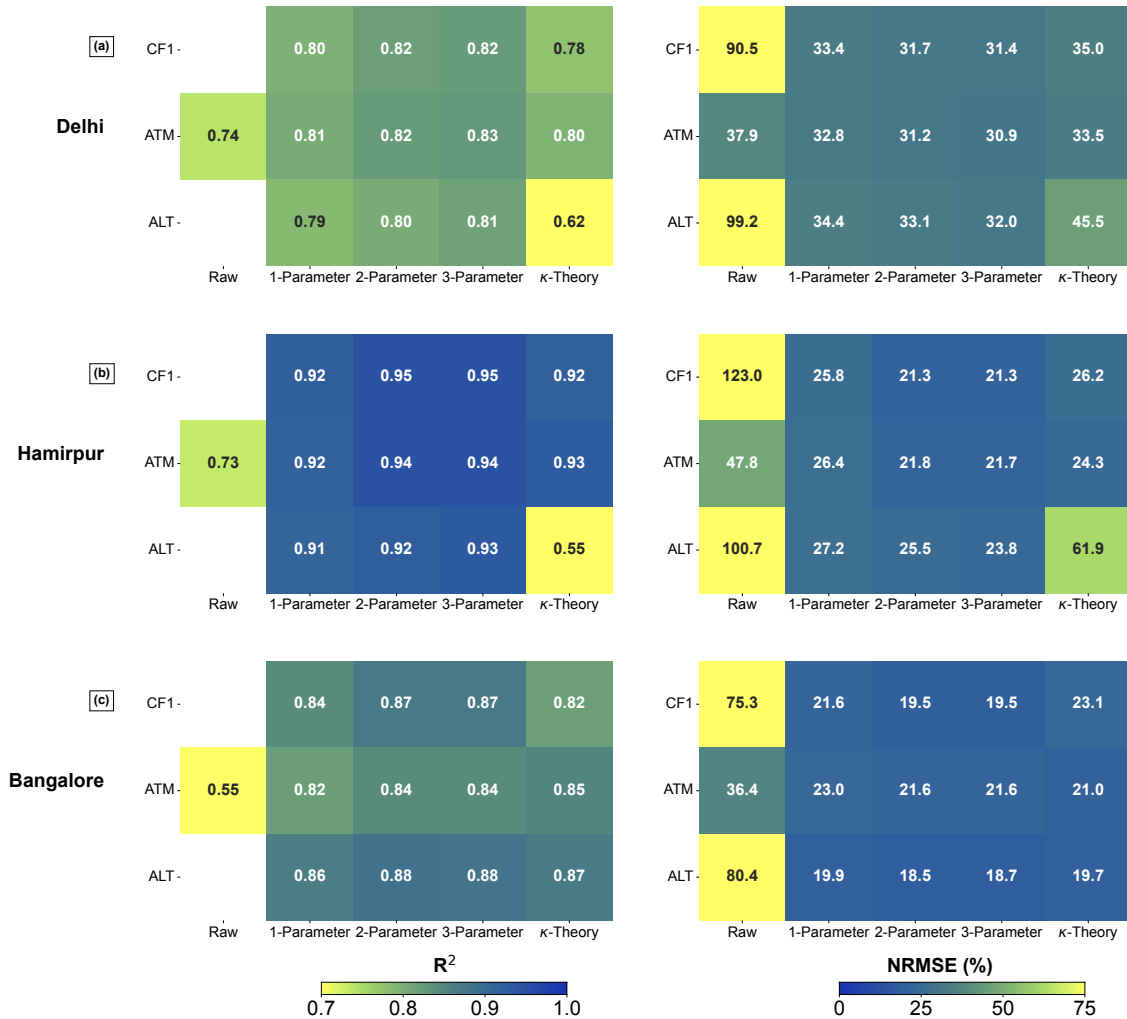


**Figure 3.** Regression metrics,  $R^2$  (left) and NRMSE (right) for raw data, 1-parameter model, 2-parameter model, 3-parameter model, and the theory-driven hygroscopic growth model for each  $PM_{2.5}$  channel (CF1, ATM, ALT) for each site (Delhi [panel (a)], Hamirpur [panel (b)], and Bangalore [panel (c)]). The largest improvements are from the raw data to the 1-parameter model, with only marginal improvements in the 3-parameter and theory-driven models.

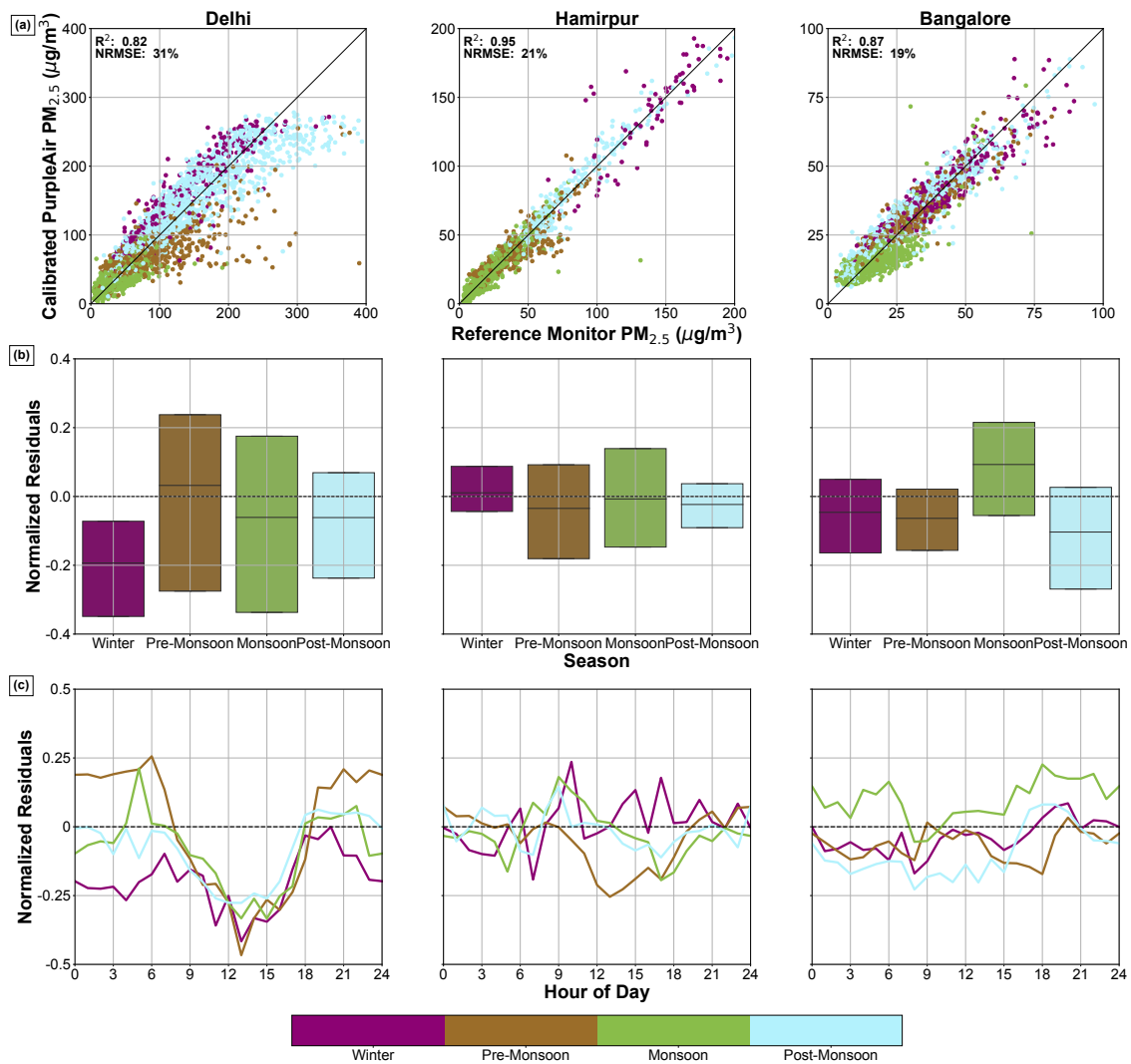


**Figure 4.** Scatter plots of the best-performing 2-parameter annual models for each of the sites in panel (a), with the corresponding normalized model residuals in panel (b) segregated by season and segregated by the time of day in panel (c). In panel (a), the solid line represents unity. In panels (b) and (c), the dashed line represents the normalized residual value of 0. In comparison to Fig. 2a, the normalized diurnal residuals in panel (c) are presented over a restricted y-axis, accentuating the residual structure.

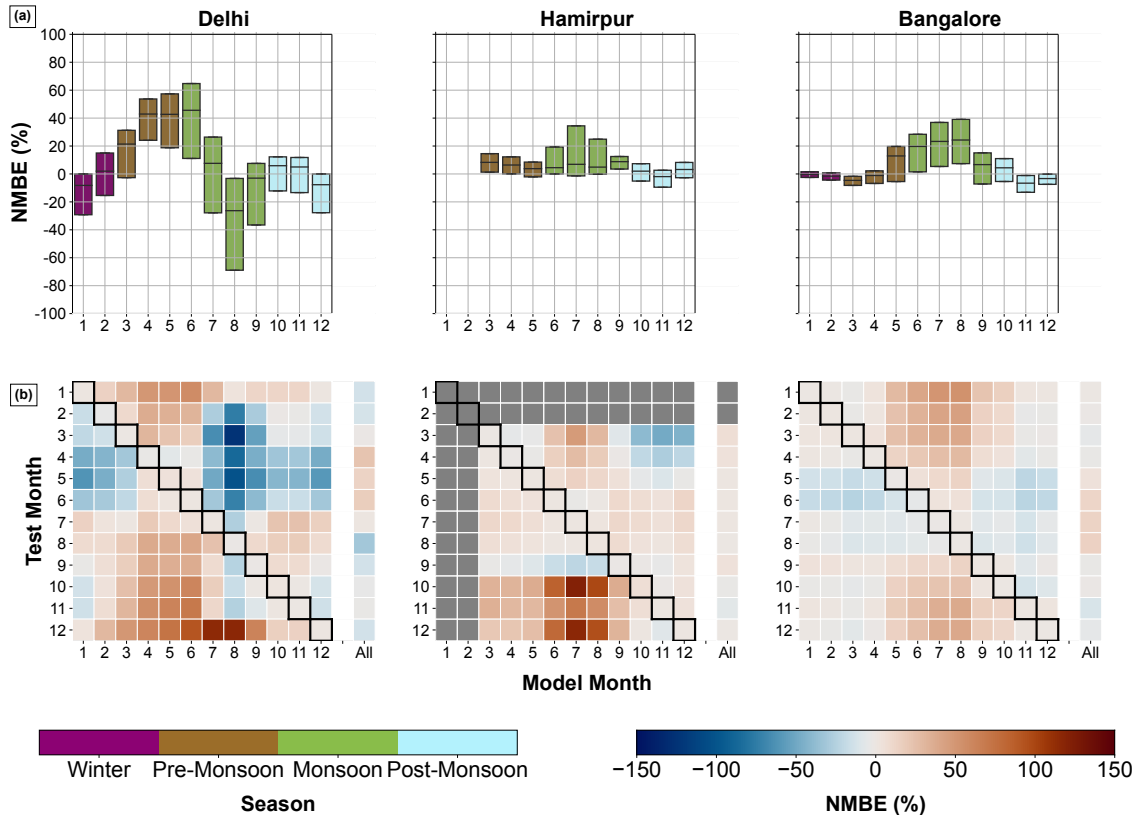


**Figure 5.** Assessment of inter-seasonal transferability of seasonal models. Panel (a) depicts box plots of the distribution of Normalized Mean Bias Error (NMBE) for a given model starting month of a 4-week rolling ordinary least-squares (ROLS) model on all other windows. The bottom, solid line, and top of the boxes represent the 25<sup>th</sup>, 50<sup>th</sup>, and 75<sup>th</sup> percentiles respectively. Panel (b) presents the median NMBE of a 4-week ROLS model trained to start in the month (colored by season) on the x-axis and evaluated on all other windows as binned by starting month on the y-axis. Gray boxes represent months without sufficient data. Models trained in the Pre-Monsoon underpredicted in other seasons, contrary to the typical pattern of overprediction – this pattern is consistent at Delhi and Hamirpur. As a point of comparison, we present the performance of our long-term calibration in individual months at each site in column (b) titled “All.” Consistent with our observation that 4-week models trained in a single month generally do not perform as well in other months.

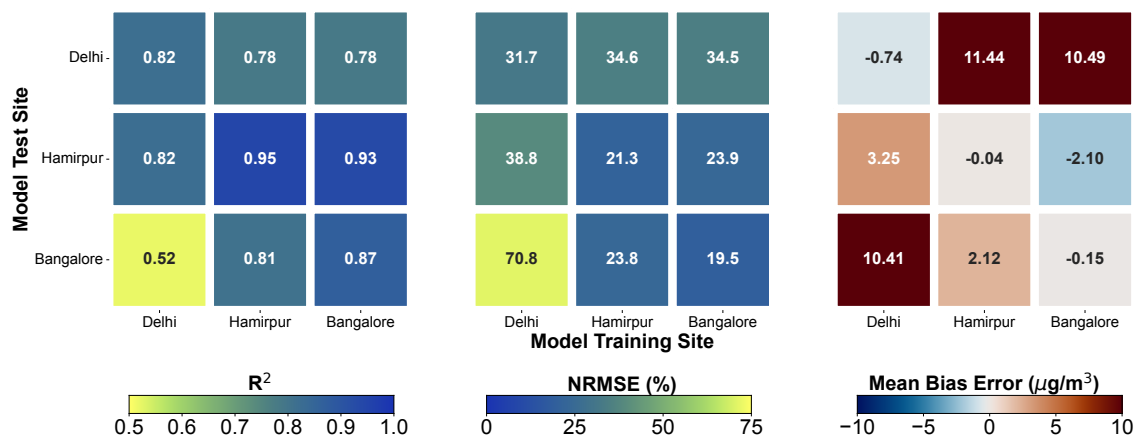


**Figure 6.** Assessment of site-wise transferability of annual models. Performance evaluation metrics of Eq. (2-4) with the training site on the x-axis and the test site on the y-axis. Metrics are Coefficient of Determination ( $R^2$ ) (left), Normalized Root Mean Square Error (NRMSE) (center), and Mean Bias Error (right). For each metric, the diagonal pattern of the best performance from upper left to lower right illustrates how calibration models perform best in the locations where they are trained. At each site, we compute performance metrics by comparing the calibration model output to an independent test set that was held out from model training. This finding illustrates how regional differences in meteorology and aerosol composition can limit the transferability of calibration relationships. Of note, the calibration model trained in Delhi performed quite poorly in Bangalore.

	Delhi	Hamirpur	Bangalore
BAM 1020/1022 PM <sub>2.5</sub> ( $\mu\text{g}/\text{m}^3$ )			
p <sub>10</sub>	23.0	10.6	10.8
p <sub>25</sub>	39.0	17.9	15.3
p <sub>50</sub>	71.0	34.3	21.8
p <sub>75</sub>	142.0	67.4	30.8
p <sub>90</sub>	237.0	125.4	42.1
PA-II CF1 PM <sub>2.5</sub> ( $\mu\text{g}/\text{m}^3$ )			
p <sub>10</sub>	31.0	18.1	12.7
p <sub>25</sub>	52.2	31.3	18.1
p <sub>50</sub>	117.0	63.4	31.0
p <sub>75</sub>	243.0	124.3	52.9
p <sub>90</sub>	375.0	218.0	74.5
PA-II ATM PM <sub>2.5</sub> ( $\mu\text{g}/\text{m}^3$ )			
p <sub>10</sub>	30.4	18.1	12.7
p <sub>25</sub>	43.0	30.2	18.1
p <sub>50</sub>	83.8	47.0	30.0
p <sub>75</sub>	180.0	82.7	42.4
p <sub>90</sub>	285.0	146.7	51.3
PA-II RH (%)			
p <sub>10</sub>	20.6	29.8	34.2
p <sub>25</sub>	29.6	44.1	48.0
p <sub>50</sub>	41.0	62.9	62.9
p <sub>75</sub>	48.5	77.4	73.8
p <sub>90</sub>	53.1	85.7	78.6
PA-II Temperature ( $^{\circ}\text{C}$ )			
p <sub>10</sub>	18.7	17.2	23.7
p <sub>25</sub>	22.8	24.5	25.0
p <sub>50</sub>	29.2	30.6	27.7
p <sub>75</sub>	35.1	35.3	32.3
p <sub>90</sub>	39.0	40.3	37.1

**Table 1.** Summary of campaign measurements (quality assured according to methods outlined in 2.4 and summarized in 3.1 - 3.3) including 10<sup>th</sup> percentile (p<sub>10</sub>), 25<sup>th</sup> percentile (p<sub>25</sub>), 50<sup>th</sup> percentile (p<sub>50</sub>), 75<sup>th</sup> percentile (p<sub>75</sub>), and 90<sup>th</sup> percentile (p<sub>90</sub>) for the campaign periods (Delhi: 2018 July – 2020 April, Hamirpur: 2020 January – 2021 January, Bangalore: 2019 June – 2020 August)

	CF1	ATM	ALT
<i>Delhi</i>	$PM_{2.5}$	$PM_{2.5}$	$PM_{2.5}$
	RH	$RH^2$	$RH^2 \times T$
	$PM_{2.5} \times RH$	$PM_{2.5} \times RH^2$	$PM_{2.5}^2 \times D$
	$PM_{2.5}$	$PM_{2.5}$	$PM_{2.5}$
<i>Hamirpur</i>	RH	RH	$PM_{2.5} \times RH \times T$
	$RH^3$	$RH^2$	$PM_{2.5}^2 \times D$
	$PM_{2.5} \times T$	$PM_{2.5}^2 \times T$	$PM_{2.5}$
<i>Bangalore</i>	$PM_{2.5} \times T \times D$	$PM_{2.5}^3$	$PM_{2.5} \times RH^2$
	$PM_{2.5}^2 \times T$	$PM_{2.5}^2$	$PM_{2.5}^2 \times T$

**Table 2.** Most relevant parameters selected through Sequential Feature Selection for each PurpleAir  $PM_{2.5}$  channel by site: CF1 (“uncorrected” PurpleAir  $PM_{2.5}$ ), ATM (“atmospheric corrected” PurpleAir  $PM_{2.5}$ ), and ALT (“alternative” PurpleAir  $PM_{2.5}$  – reconstructed from modeled size distribution data). Parameters: Relative Humidity (RH), Temperature (T), and Dew Point (D).